NACA

RESEARCH MEMORANDUM

FLIGHT MEASUREMENTS OF THE LATERAL STABILITY

AND CONTROL CHARACTERISTICS OF A

HIGH-SPEED FIGHTER AIRPLANE

By H. L. Crane, A. R. Beckhardt, and C. E. Matheny

Langley Aeronautical Laboratory
Langley Field, Va.

NATIONAL ADVISORY COMMITTEE
FOR AERONAUTICS

WASHINGTON
September 23, 1952

NATIONAL ADVISORY COMMITTEE FOR AERONAUTICS

RESEARCH MEMORANDUM

FLIGHT MEASUREMENTS OF THE LATERAL STABILITY

AND CONTROL CHARACTERISTICS OF A

HIGH-SPEED FIGHTER AIRPLANE

By H. L. Crane, A. R. Beckhardt, and C. E. Matheny

SUMMARY

This paper presents the results of a brief flight investigation
of the lateral stability and control characteristics of a high-speed
fighter airplane. The tests reported herein were intended to be pre-
liminary to a flight investigation to measure the lateral-stability
derivatives. The variation of rudder and aileron deflection, pedal
force, and lateral-force coefficient with angle of sideslip are pre-
sented for Mach numbers up to 0.815 at an altitude of 10,000 feet and
for Mach numbers up to 0.84 at an altitude of 30,000 feet. Values of
the rate of change of lateral-force coefficient with angle of sideslip
determined from the flight tests and corrected for the rudder deflec-
tion required for trim agreed with wind-tunnel results. Brief measure-
ments of the damping of the controls-free lateral oscillations showed
that the cycles to damp to half amplitude varied from approximately 1.6
to 2.1 at an altitude of 10,000 feet and from 2.6 to 3.6 at 30,000 feet.
It was found that the rudder tended to float against the relative wind
for small angles of sideslip and that this airplane was an example of
one in which at least part of the unsatisfactory lateral damping char-
acteristics appeared to be due to rudder snaking. Correlation between
measured damping of the controls-free lateral oscillation and calculated
damping of the controls-fixed lateral oscillation appeared to be good when
allowance was made by an approximate method for the effect of the rud-
der motion. The evidence of agreement shown by the method of compari-
son used in the analysis does not necessarily indicate that all the
stability derivatives and mass characteristics assumed in the theoret-
ical analysis are correct, however, since there is the possibility of
compensating errors.

INTRODUCTION

The Flight Research Division of the NACA is conducting an investigation of the dynamic lateral stability characteristics of several modern, high-speed aircraft. One phase of this investigation is concerned with the measurement in flight of the lateral-stability derivatives of representative modern fighter aircraft. The present paper discusses preliminary results of a flight investigation of the lateral stability characteristics of one fighter airplane.

At the initiation of the test program it was decided to make several flights to investigate the general lateral handling qualities of the test aircraft. It was felt that these tests, made mostly at high subsonic speeds, were a logical starting point preceding the actual measurement of the lateral-stability derivatives of the test airplane.

During the course of the service acceptance trials, many of the handling qualities of this airplane were measured in the stability and control phase of the tests. The service tests included an evaluation of the handling qualities and sufficient quantitative data were obtained to demonstrate compliance with the requirements of SR-119B (reference 1). The tests reported herein were made to permit a more thorough analysis of several phases of the lateral handling qualities.

Because the actual measurement of stability derivatives has not yet been obtained, this paper is preliminary in nature and includes only the test data of interest obtained to date.

DESCRIPTION OF AIRPLANE

The test airplane was a single-place, two-engine, jet-propelled fighter with an unswept low wing and a conventional tail configuration. Stressed metal skin construction is utilized throughout with all lifting surfaces being of the full cantilever type. The airplane is equipped with split flaps and speed brakes. There are trim tabs on all control surfaces. A three-view drawing of the test airplane is shown in figure 1 and the general specifications of the airplane are tabulated in table I. The test airplane was modified by the removal of the ammunition cases and one of the 20-millimeter guns to provide space for the instrumentation necessary for the tests. The test airplane had a gross weight of 15,956 pounds with full service, pilot, and loaded instruments with the center of gravity located at 25.5 percent of the mean aerodynamic chord.

The aileron control system of the test airplane is a push-pull rod system with two completely independent hydraulic boost systems, one on each aileron. A bench mock-up of the aileron boost system was constructed of spare parts to provide a test facility for the observance of the operating characteristics of a typical service booster system. During these tests the static boost ratio of the aileron control system was measured and the results are shown in figure 2. The static boost ratio was determined to be approximately 40:1 with a break-out force of approximately 3 pounds. Additional information on the airplane's control-system characteristics is given in table I.

INSTRUMENTATION

Standard NACA recording instruments were used to measure the following quantities: indicated airspeed, pressure altitude, control positions, control forces, sideslip angle, angle of attack, angular velocities, angular accelerations, and the normal, transverse, and longitudinal accelerations. These quantities were measured with respect to the body axes. It should be noted that the lateral acceleration was measured in the cockpit approximately 6 feet ahead of the center of gravity and was not corrected for the effect of this displacement. The airspeed and altitude measurements were made with a Kollsman high-speed pitot-static tube mounted approximately 1 chord ahead of the right wing tip. Calibration of similar installations has indicated that this type of installation would probably have a position error in the static pressure of less than one-half of 1 percent throughout the test speed range. Airspeed as used in this paper is indicated airspeed and is not corrected for position error. The recording sideslip vane and angle-of-attack vane were mounted on a boom approximately one maximum fuselage diameter ahead of the nose.

SYMBOLS

β angle of sideslip, degrees

δ_r rudder deflection, degrees

δ_{r_o} amplitude of rudder oscillation, degrees

δ_a aileron deflection, degrees

F_p rudder pedal force, pounds

C_Y lateral-force coefficient

C_{Y_β} rate of change of lateral-force coefficient with angle
              of sideslip, per radian

$C_{Y_{\delta_r}}$ rate of change of lateral-force coefficient with rudder
              deflection, per degree

C_L lift coefficient

d logarithmic decrement of lateral oscillation

P period of lateral oscillation, seconds

$T_{1/2}$ time to damp to one-half amplitude, seconds

$C_{1/2}$ cycles to damp to one-half amplitude

W work, foot-pounds

N_{δ_r} yawing moment due to rudder deflection, foot-pounds per
              degree $\left(C_{N_{\delta_r}} qSb \right)$

C_N yawing-moment coefficient

$C_{N_{\delta_r}}$ rate of change of yawing-moment coefficient with rudder
              deflection, per degree

q dynamic pressure, pounds per square foot

S wing area, square feet

b wing span, feet

M Mach number

ϕ angle of bank, degrees

ψ angle of yaw, degrees

ψ_0 amplitude of yawing oscillation, degrees

θ phase angle between rudder deflection and angle of yaw

I_Z moment of inertia about z-axis, slug-feet^2

ΔKE	increment of kinetic energy, foot-pounds
C_h	hinge-moment coefficient
C_{h_δ}	rate of change of hinge-moment coefficient with control deflection, per degree
C_{h_ψ}	rate of change of hinge-moment coefficient with angle of yaw, per degree
C_{h_α}	rate of change of hinge-moment coefficient with angle of attack, per degree
$pb/2V$	flight-path helix angle, radians
p	rolling angular velocity, radians per second
V	true airspeed, feet per second
V_i	indicated airspeed, miles per hour or knots
V_e	equivalent airspeed, miles per hour or knots as defined in reference 2
ω	angular frequency of periodic function, radians per second

RESULTS AND DISCUSSION

Control-free lateral oscillations.- The damping and period measured at several Mach numbers and altitudes is superposed on the criterion of SR-119B in figure 3 and indicates that, with the controls free, the damping of the test airplane was marginally unsatisfactory with respect to meeting the handling-qualities requirements at 10,000 feet altitude and definitely unsatisfactory at 30,000 feet altitude. These tests were made in the clean condition with power for level flight. The oscillations were initiated by releasing the airplane from steady sideslips. Typical time histories of the lateral oscillations are presented in figure 4. Figures 4(a) and 4(b) present all the measured quantities while figure 4(c) presents a photographic copy of the records of some of the more important parameters to show them in more detail.

The characteristics of the damping of the lateral oscillation of the test airplane are shown in figure 5 in another form. This figure is an example (not taken from fig. 4(c)) of the logarithmic variation

of the double amplitude of the yawing velocity with time. In several
runs a nonlinear logarithmic variation of amplitude with time was
obtained. Such a nonlinear variation can be caused by slight roughness
in the air, but in some cases records of this type were obtained in
apparently smooth air. This type of nonlinear variation when measured
in smooth air could be caused by small aileron or rudder motions or by
nonlinear stability derivatives. Figure 5 is an example of the decrease
in damping at small amplitudes obtained during a run in apparently
smooth air.

The data of figure 3 have been replotted in figure 6 in terms of
the logarithmic decrement of the lateral oscillation to indicate the
variation of the damping with Mach number. The logarithmic decrement
is obtained from the slope of the linear portion of the curve in log-
arithmic plots, such as figure 5, and is the $\log_e$ of the ratio of
successive peak amplitudes during a lateral oscillation. The logarith-
mic decrement d is related to the time to damp to half amplitude by
the following relationship:

$$d = \frac{0.693P}{T_{1/2}} = \frac{0.693}{C_{1/2}}$$

As indicated in figure 6, the value of the logarithmic decrement was
approximately 0.42 at $M = 0.35$, 0.34 at $M = 0.50$, and 0.35 at $M = 0.70$
for an altitude of 10,000 feet.

Also plotted in figure 6 are the results of some analytical cal-
culations of the damping for the test airplane. These calculated
values of damping of the lateral oscillation were based on inertia
values supplied by the manufacturer corrected for fuel consumption and
instrumentation, and stability derivatives estimated by the methods of
references 3 and 4. These controls-fixed calculations indicate a
higher degree of damping than was measured with controls free.

Examination of the time history presented in figure 4(c) indicates
that the rudder has a tendency to float against the relative wind
(increasing right sideslip resulting in increasing right rudder deflec-
tion) over the range of tail angles of attack encountered in these maneu-
vers. The rudder deflection lagged the angle of yaw by about 20° with
the result that there was a tendency to feed energy into the oscillation.
This type of controls-free lateral oscillation is an example of rudder
snaking, but in this case the influence of the rudder is sufficient only
to reduce the damping of the Dutch roll oscillation rather than to pro-
duce a constant amplitude motion.

Since the flight test data indicated that the position of the rudder was not constant during the lateral oscillations, an estimate was made of the magnitude of the effect that rudder motion would have on the computed logarithmic decrement. The work done per cycle by a harmonically varying force upon a harmonic motion of the same frequency in a system assumed to have one degree of freedom can be written as

$$W = \pi \delta_{r_0} N_{\delta_r} \psi_0 \sin \theta \tag{1}$$

where, for the case under consideration,

$\delta_{r_0} N_{\delta_r}$ amplitude of yawing moment due to rudder motion

$$\left(\delta_{r_0} \left(C_{n_{\delta_r}} qSb \right) \right) \quad \left(C_{n_{\delta_r}} \text{ obtained from wind-tunnel data} \right)$$

ψ_0 amplitude of yawing displacement (obtained from yawing-velocity recorder)

θ phase angle between forcing function δ_r and displacement ψ

In this analysis it was necessary to assume that for the cycle considered the airplane and rudder were oscillating at a constant amplitude equal to the average of successive maximum (positive) and minimum (negative) amplitudes.

The work per cycle due to the rudder oscillation was then compared to the loss in kinetic energy per cycle which can be computed from the following relationship:

$$\Delta KE = \frac{I_Z}{2} \left(\psi_1^2 - \psi_2^2 \right) \omega^2 = 2\pi^2 \frac{I_Z}{P^2} \left(\psi_1^2 - \psi_2^2 \right) \tag{2}$$

in which ψ_1 and ψ_2 represent the maximum yaw angles at corresponding points on two successive cycles. For example, it can be determined from the time history of figure 4(c) that the rudder is oscillating in the cycle indicated with an average amplitude of approximately 0.27° and the airplane is oscillating in yaw with an average amplitude of approximately 1.20°. The phase angle between the rudder displacement and the airplane yawing displacement is approximately 20° with the rudder lagging. The work per cycle for this example is then

$$W = \pi \left[(-0.27)(-0.0014)(281)(294.1)(41.74) \right] \frac{1.20}{57.3} \sin 20^\circ = 29 \text{ foot-pounds}$$

The loss in kinetic energy for this example is approximately

$$\Delta KE = 2\pi^2 \left(\frac{38,000}{(1.70)^2}\right)\left[\left(\frac{1.32}{57.3}\right)^2 - \left(\frac{0.96}{57.3}\right)^2\right] = 65 \text{ foot-pounds}$$

The work input from the rudder motion and the loss in kinetic energy involve a gross energy of approximately 94 foot-pounds in this example. Recomputing the value of ψ_2 from equation (2) for this energy change gives an adjusted value of ψ_2 for the controls-fixed case of approximately 0.74°. The log decrement is correspondingly adjusted from the value of 0.334 at $M = 0.51$ in figure 6 to $d = \log_e \frac{1.32}{0.74} = 0.58$ which is in good agreement with the controls-fixed calculated value of 0.60. This good agreement was obtained on four different runs but the apparent agreement should be viewed with caution not only in view of the assumptions made in correcting the measured log decrements but in view of the fact that the calculated values may be in error due to errors in the assumed mass characteristics or in the values of the stability derivatives used in the calculations.

It would be desirable to continue this phase of the investigation and to measure the damping characteristics throughout the altitude and Mach number range of the test aircraft with the control surfaces fixed.

Sideslip characteristics.- The sideslip data which gave measurements of directional stability (variation of rudder angle and force with sideslip angle), dihedral effect (variation of aileron angle and force with sideslip angle), and the side-force characteristics (variation of angle of bank with angle of sideslip) are shown in figures 7 and 8. The data are presented for the two test altitudes of approximately 10,000 and 30,000 feet for a Mach number range from 0.20 to 0.84. The data of figure 7 were obtained during continuous gradually increasing sideslips to the right and to the left. The rate of change of sideslip was at approximately $1/2^\circ$ per second. The data of figure 8 were obtained during steady sideslips.

The directional stability as indicated by the curves of rudder angle and force was always positive. The directional-stability parameter $\partial\delta_r/\partial\beta$ and the directional-force characteristics as measured by $\partial F_p/\partial\beta$ measured through zero sideslip are plotted against Mach number for the two test altitudes in figure 9(a). In preparing figure 9 the steady sideslip data of figure 8 as well as the results of the gradually increasing sideslips of figure 7 were used. At

10,000 feet, the parameter $\partial\delta_r/\partial\beta$ increased from about 1.2 at low speeds to about 2.4 at a Mach number of 0.74. Further increase in Mach number to 0.82 resulted in a decrease in $\partial\delta_r/\partial\beta$ to about 1.8. At 30,000 feet, $\partial\delta_r/\partial\beta$ was approximately 1.3 and essentially constant up to a Mach number of 0.70. From a Mach number of 0.70 to 0.84, $\partial\delta_r/\partial\beta$ increased slightly and then decreased to a value of about 1.3 again. Rudder deflection was determined from the position of a control pushrod in the after portion of the fuselage and was therefore affected by twist of the rudder or distortion of the linkage. Because of the large difference in dynamic pressure for the two test altitudes at a given Mach number, it seemed likely that the differences between the values of $\partial\delta_r/\partial\beta$ measured at 10,000 feet and at 30,000 feet were due in large measure to distortion in the rudder control system and airframe. Figure 9(b) which is a plot of the parameters of figure 9(a) against dynamic pressure bears out this theory. Below the point where Mach number effects are evident the curves are approximately linear and the values approximately equal for the two altitudes.

The dihedral effect as measured by the variation of aileron angle with sideslip which is also presented in figure 9 was approximately constant up to a Mach number of 0.80 where the sharp increase in $\partial\delta_a/\partial\beta$ indicates an increase in the rolling moment due to sideslip and/or a decrease in aileron effectiveness. There is a nonlinearity or offset near zero sideslip in the variation of aileron deflection with angle of sideslip for the gradually increasing sideslip data of figure 7. This offset is probably due to the aileron deflection necessary to produce the slow rolling velocity in the gradually increasing sideslips. The values of $\partial\delta_a/\partial\beta$ were therefore measured at large enough sideslip angles so that the measured slope was not dependent on the fairing in the region of the offset. It was felt that the slopes measured in this manner would be more representative of the characteristics of the airplane.

At the lower test Mach numbers the variation of elevator position and control force with angle of sideslip was small. However, at Mach numbers above approximately 0.8 the variation of elevator control force with sideslip became erratic with abrupt changes of as much as 20 pounds.

The angle of bank was always in the same direction as the angle of sideslip. The angle of bank required to hold a steady sideslip was generally small at low speeds $\left(\dfrac{\phi}{\beta} \approx 0.5\right)$. Because the side force for a given sideslip angle varies approximately as the dynamic pressure, the angles of bank required increased rapidly at the higher test speeds.

In wind-tunnel tests the side-force derivative C_{Y_β} is measured by yawing the model with the rudder in neutral. In flight the pilot must deflect the rudder to produce a steady sideslip and therefore C_{Y_β} cannot be measured directly. To obtain a comparison of wind-tunnel and flight measurements of side-force characteristics, the values of the side-force derivative measured in flight were corrected for the side force due to rudder deflection by using wind-tunnel data to obtain values of $C_{Y_{\delta_r}}$. The variation of the side-force derivative C_{Y_β} with Mach number as computed from the variation of angle of bank with sideslip angle in sideslips is presented in figure 10. The value of the side-force derivative with rudder deflected for trim is also plotted in figure 10.

The side-force derivative C_{Y_β} was essentially constant with increasing Mach number up to a Mach number of 0.75. At low Mach numbers C_{Y_β} was approximately -0.63 increasing to about -0.70 at a Mach number of 0.75. From $M = 0.75$ to 0.84, C_{Y_β} decreased to a value of about -0.48. The values of C_{Y_β} obtained from the flight test data are in good agreement with the values measured in wind-tunnel tests as shown in figure 10.

Rudder control characteristics.- The rudder control characteristics measured in abrupt rudder kicks are shown in figure 11. At 10,000 feet, $V_i \approx 240$ miles per hour, a sideslip angle of about 20° resulted from an abrupt maximum rudder deflection of about 17°. At 30,000 feet, $V_i \approx 335$ miles per hour, a maximum sideslip angle of about 8° resulted from a rudder deflection of about 6° which was limited to this value by the large control force required. As shown in figure 11(a), no appreciable difference in the rudder control characteristics was noted at landing speeds between the clean condition and the landing condition. Left rudder force was always required for left-rudder deflections and right rudder force for right rudder deflection. No reversal of rudder forces ever occurred.

Rudder hinge-moment characteristics.- The rudder hinge-moment characteristics measured in abrupt rudder kicks are presented in figure 12. The data were calculated from time histories of rudder kicks made at both 10,000 and 30,000 feet from $M = 0.20$ to $M = 0.77$.

The variation of hinge moment due to rudder deflection as a function of rudder deflection presented in figure 12(a), which was obtained from

the initial portions of the step maneuvers during which the sideslip angle was essentially constant, is linear up to a rudder deflection of about ±10°. The slope C_{h_δ} is -0.0113 through this range of rudder deflection. For rudder deflections above 10° a possible increase in C_{h_δ} is indicated by the data of figure 12(a).

The hinge moment due to change in sideslip alone was determined from the second portion of the rudder-kick time histories during which the rudder deflection was held constant while the sideslip gradually increased. A correction was applied for any inadvertent motion of the rudder. As noted in the section on control-free lateral oscillations, there was evidence during several of the lateral oscillations of a tendency for the rudder to float against the relative wind. This occurrence would indicate a negative value for C_{h_β}, which can be considered approximately equivalent to a positive value of C_{h_α} if the sidewash is considered to be small, at small angles of sideslip $\left(\beta \gtrless 5^\circ\right)$. To assist in the fairing at small angles of sideslip of the curve of hinge-moment coefficient against sideslip, shown in figure 12(b), values of the variation of C_h with β were calculated from the ratio of rudder trailing angle to sideslip angle in rudder-free lateral oscillations. It was found that the maximum value of C_h caused by the tendency to float against the relative wind was approximately 0.004 at 2° or 3° of sideslip.

Rolling characteristics.- The variation of rolling effectiveness with aileron deflection (boost on) at the test altitudes of 10,000 and 30,000 feet is presented in figure 13. Within the capability of the booster the required control force and the change in rolling velocity obtained in abrupt rudder-fixed aileron rolls from wings level flight varied smoothly with aileron deflection throughout the Mach number range tested. The pilot did not consider the 2- or 3-pound breakout force to be objectionable. It should be noted that the abrupt increase in control force occurs when the capability of the aileron booster is exceeded. The rolling effectiveness with the flaps and gear down was checked at 5,000 feet (fig. 13(c)) and the characteristics were found to be satisfactory.

The variation of the aileron rolling-effectiveness parameter $pb/2V$, as limited by full aileron deflection or 30-pound control force (boost on), with airspeed is presented in figure 14. Figure 14 also shows the corresponding variation of rolling velocity, control force, and total aileron deflection. The rolling performance of the test airplane exceeds the requirements of SR-119B up to approximately 315 knots $\left(V_i\right)$ at the test altitude of 10,000 feet. From 315 knots to 410 knots, the helix angle obtained decreases from about 0.09 to 0.06. Although the rolling

requirements at 30,000 feet are not specified, the test airplane sat-
isfied the low-altitude requirements up to an indicated airspeed of
approximately 200 knots. From 200 knots to the maximum test speed of
approximately 275 knots the rolling effectiveness parameter pb/2V for
a 30-pound aileron control force decreased from about 0.09 to 0.07.

CONCLUSIONS

The following conclusions may be drawn from the present flight
investigation of the lateral stability and control characteristics of
a high-speed fighter airplane reported herein:

1. The damping of the controls-free lateral oscillation of the
test airplane was marginal and did not meet the requirements of SR-119B.
The cycles to damp to half amplitude varied from approximately 1.6 to 2.1
at an altitude of 10,000 feet and from 2.6 to 3.6 at 30,000 feet. There
was evidence (for sideslip angles less than 5°) of a positive value of
C_{h_α}, the hinge-moment coefficient due to angle of attack, which corre-
sponds to a tendency for the rudder to float against the relative wind.
This airplane is an example of one in which at least part of the unsat-
isfactory lateral damping characteristics appears to be due to rudder
snaking.

2. The directional stability of the test airplane was always
positive.

3. The dihedral effect as indicated by the parameter $\partial \delta_a / \partial \beta$ was
positive and essentially constant up to Mach number of 0.80 above which
$\partial \delta_a / \partial \beta$ increased abruptly.

4. The side-force derivative C_{Y_β} was approximately constant
with increasing Mach number up to M = 0.75. From M = 0.75 to M = 0.84,
C_{Y_β} decreased from about -0.70 to about -0.48. The values of C_{Y_β}
derived from the flight test data are in good agreement with wind-tunnel
values.

5. The value of C_{h_δ}, the hinge-moment coefficient due to rudder
deflection, was linear up to a rudder deflection of approximately $\pm 10^\circ$
and was equal to approximately -0.0113 with an unbalancing tab ratio
of 1.4:1.

6. The rolling performance of the test airplane exceeds the require-
ments of SR-119B with the aileron boost on at 10,000 feet up to

approximately 315 knots. From 315 knots to 410 knots there is a decrease in rolling performance as indicated by the decrease in helix angle from 0.09 to 0.06.

Langley Aeronautical Laboratory
       National Advisory Committee for Aeronautics
              Langley Field, Va.

REFERENCES

1. Anon.: Specification for Flying Qualities of Piloted Airplanes. NAVAER SR-119B, Bur. Aero., June 1, 1948.

2. Aiken, William S., Jr.: Standard Nomenclature for Airspeeds with Tables and Charts for Use in Calculation of Airspeed. NACA Rep. 837, 1946. (Supersedes NACA TN 1120.)

3. Campbell, John P., and McKinney, Marion O.: Summary of Methods for Calculating Dynamic Lateral Stability and Response and for Estimating Lateral Stability Derivatives. NACA TN 2409, 1951.

4. Fisher, Lewis R.: Approximate Corrections for the Effects of Compressibility on the Subsonic Stability Derivatives of Swept Wings. NACA TN 1854, 1949.

TABLE I

GENERAL SPECIFICATIONS OF THE AIRPLANE

Engines:
   Type . . . . Westinghouse 24C-4B turbo-jet
   Normal static thrust at sea level, lb 2620
   Rated normal, rpm 11,800

Wing:
   Total area, sq ft 294.09
   Span, ft 41.62
   Mean aerodynamic chord, ft 7.36
   Aspect ratio 5.89
   Taper ratio 0.52
   Root chord, ft 8.41
   Tip chord, ft 4.33
   Incidence to fuselage reference
     line, deg . . . . -1/2
   Twist, deg 0
   Dihedral, deg 3
   Sweepback of leading edge, deg 0
   Airfoil root section . . . . NACA 65_1-212
   Airfoil tip section . . . . NACA 63-209

Aileron:
   Type of aileron . . . . Plain flap, 24-percent chord
   Area aft of hinge line,
     each, sq ft 9.42
   Span, ft 7.36
   Travel, deg . . . . ±20
   Balance tab area, sq ft 1.32
   Balance tab movement, (ratio adjustable
     from 0 to 1:1) deflection used, deg . . . . ±8
   Trim tab area, sq ft 0.79
   Trim tab movement, deg . . . . ±10
   Control stick movement, deg . . . . ±22.6
   Control stick length to center of grip, ft 1.2

Flaps:
   Type . . . . Split
   Total area aft of hinge line, sq ft 22.23
   Flap deflection, deg 60

TABLE I

GENERAL SPECIFICATIONS OF THE AIRPLANE - Concluded

Horizontal tail:
  Total area, sq ft 69.87
  Span, ft 18.03
  Mean aerodynamic chord, ft 3.95
  Aspect ratio 4.65
  Taper ratio 0.60
  Incidence, deg 0.42
  Dihedral of chord plane, deg 0
  Section . . . . NACA 65-011
  Type of elevator . . . . Plain flap, 30 percent chord
  Elevator root mean square chord, ft 1.135
  Elevator area aft of hinge line, total, sq ft 17.66
  Elevator span, ft 7.85
  Elevator travel, deg . . . . ±12, -18
  Trim tab area, sq ft 0.76
  Trim tab movement, deg . . . . ±20
  Spring tab area, sq ft 1.43
  Spring tab movement, deg . . . . ±30
  Tail length from leading edge of wing to 25-percent
    M.A.C. of horizontal tail, ft 18.77
  Control stick movement for full
    elevator deflection, deg . . . . -13.4, +18.6
  Control stick length to center of grip, ft 1.9

Vertical tail:
  Area, sq ft 38.36
  Span, ft 7.17
  Aspect ratio 1.34
  Section . . . . NACA 65-011
  Tail length from leading edge of wing
    to 25-percent M.A.C. of vertical tail, ft 18.96
  Rudder area, sq ft 10.13
  Rudder span, ft 7.17
  Rudder root mean square chord, ft 1.43
  Tab area, sq ft 0.91
  Rudder travel, deg . . . . ±20
  Tab travel as a trim tab, deg . . . . ±10
  Tab travel as an antibalance tab, deg . . . . -27.5, +25.8
  Pedal movement for full rudder deflection, in. . . . . ±3.25

Fuselage:
  Length, ft 40.15
  Width, ft 3.91
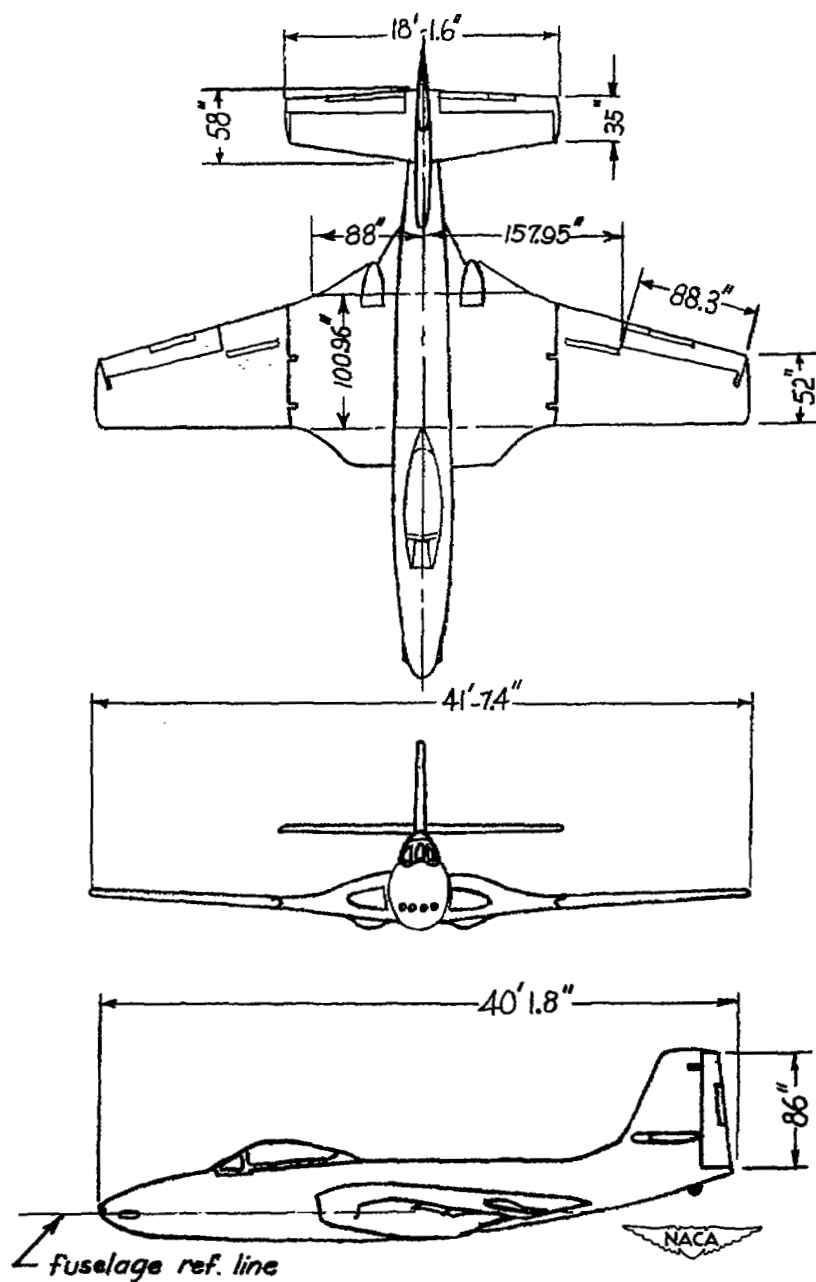
Figure 1.- Three-view drawing of the test airplane.
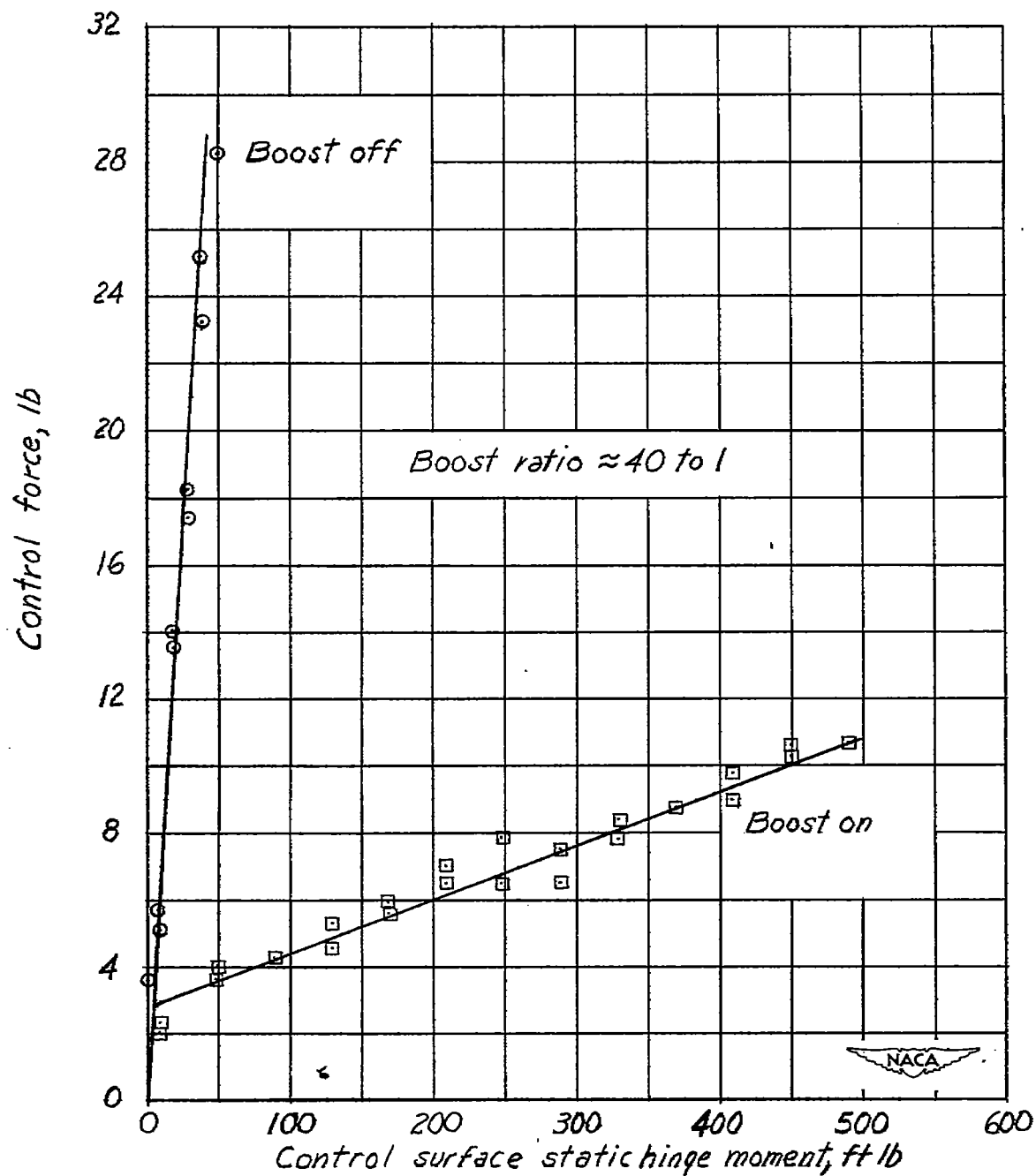
Figure 2.- The variation of aileron control force with control-surface hinge moment as measured on a bench setup.
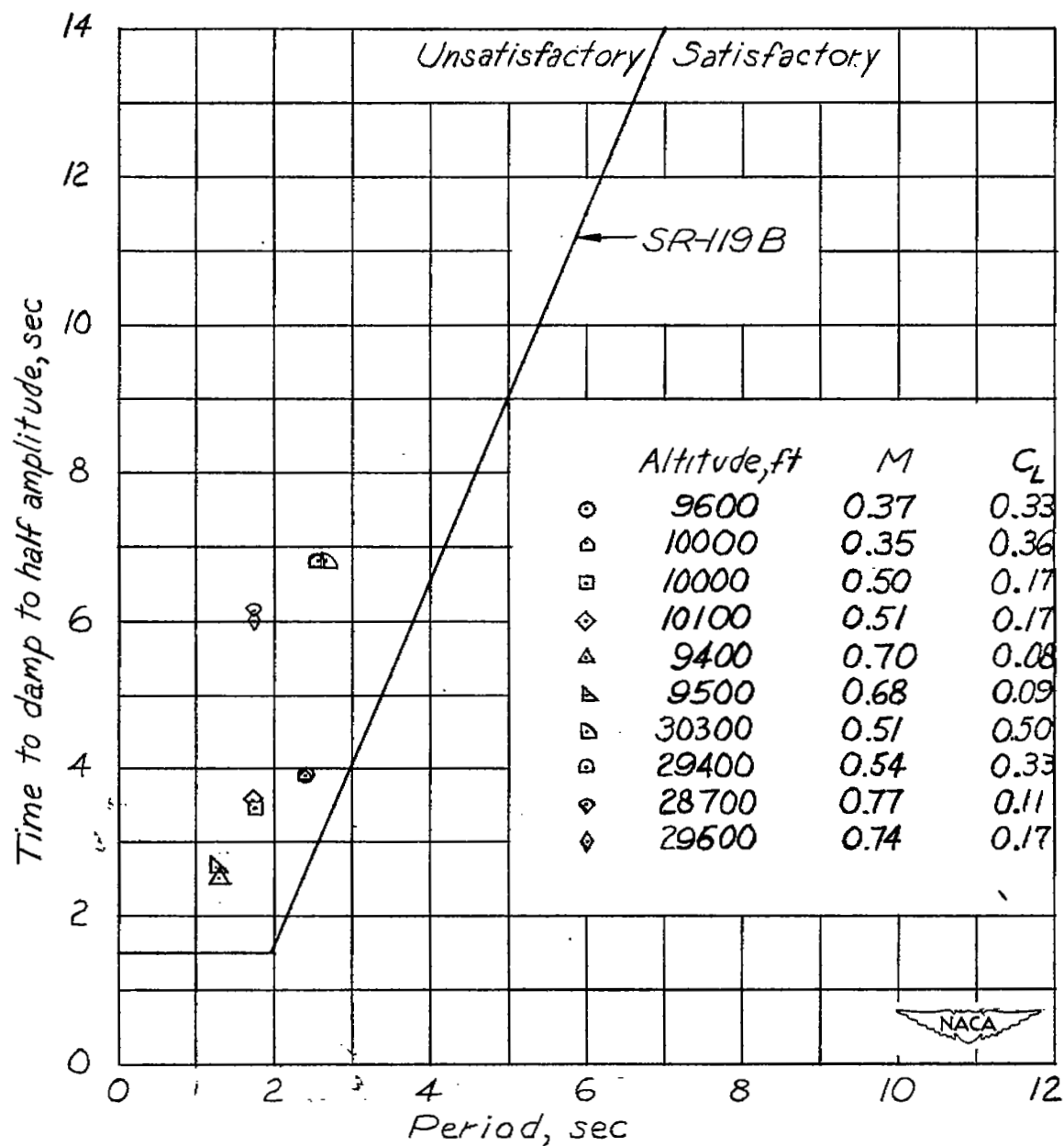
Figure 3.- Measured damping of the lateral oscillation with controls free.
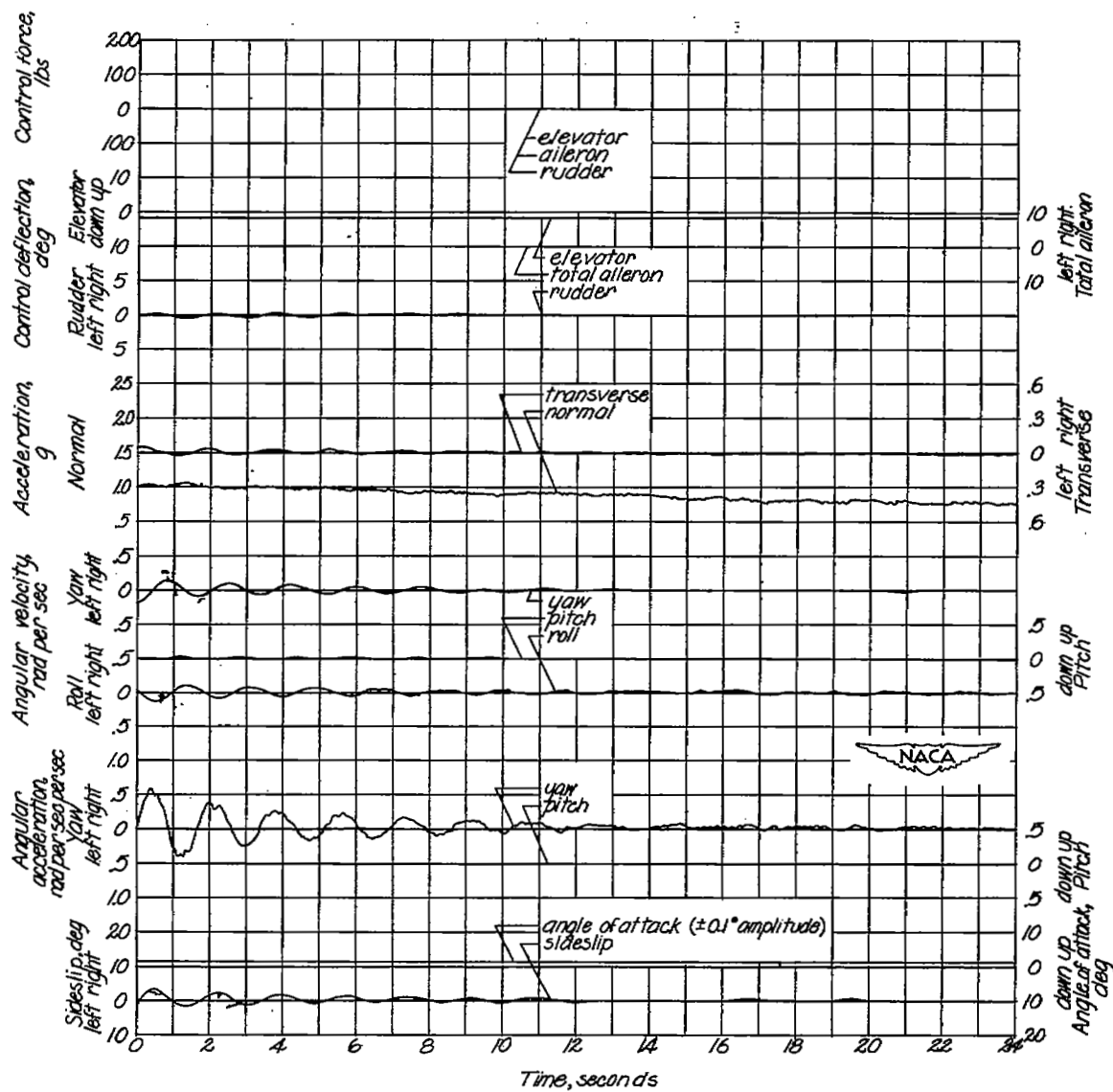
(a) M = 0.53; h_p = 10,200; V_i = 332 miles per hour; C_L = 0.17.

Figure 4.- Time histories of lateral oscillation following release from
a steady sideslip; clean condition.

no record obtained
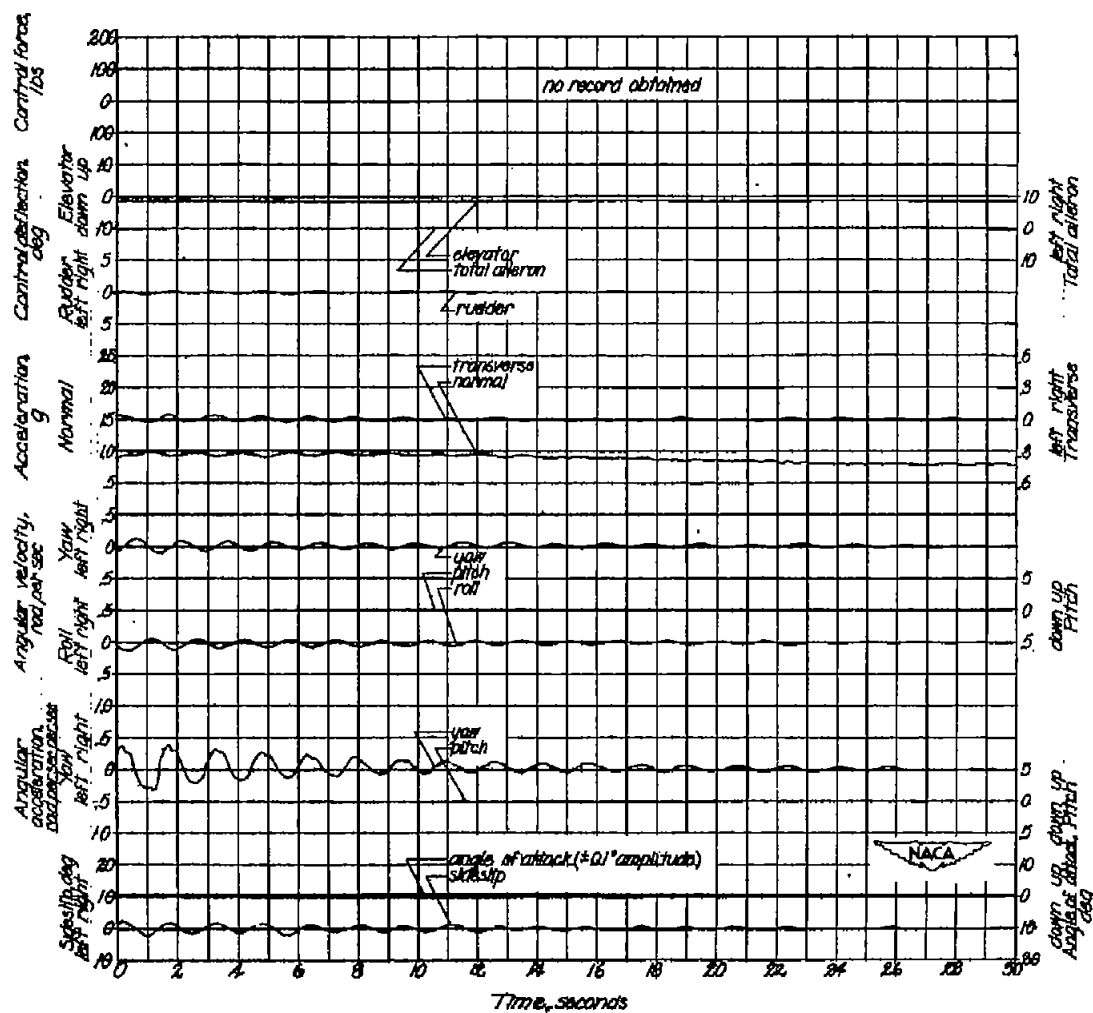
(b) M = 0.74; h_p = 29,800; V_1 = 326 miles per hour; C_L = 0.17.

Figure 4.- Continued.
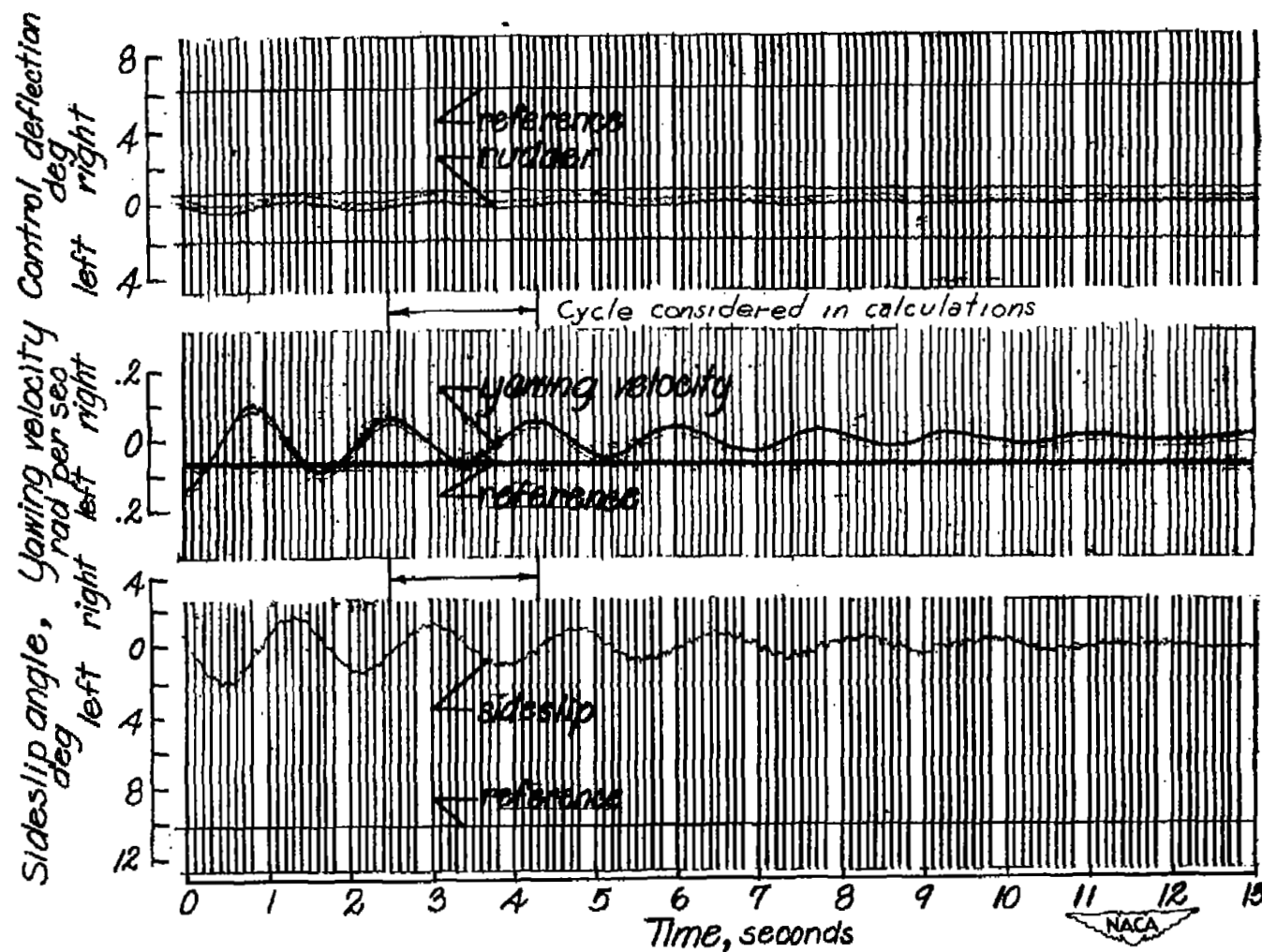
(c) $M = 0.53$; $h_p = 10,200$; $V_1 = 332$ miles per hour; $C_L = 0.17$.

Figure 4.- Concluded.

NACA RM L52B14
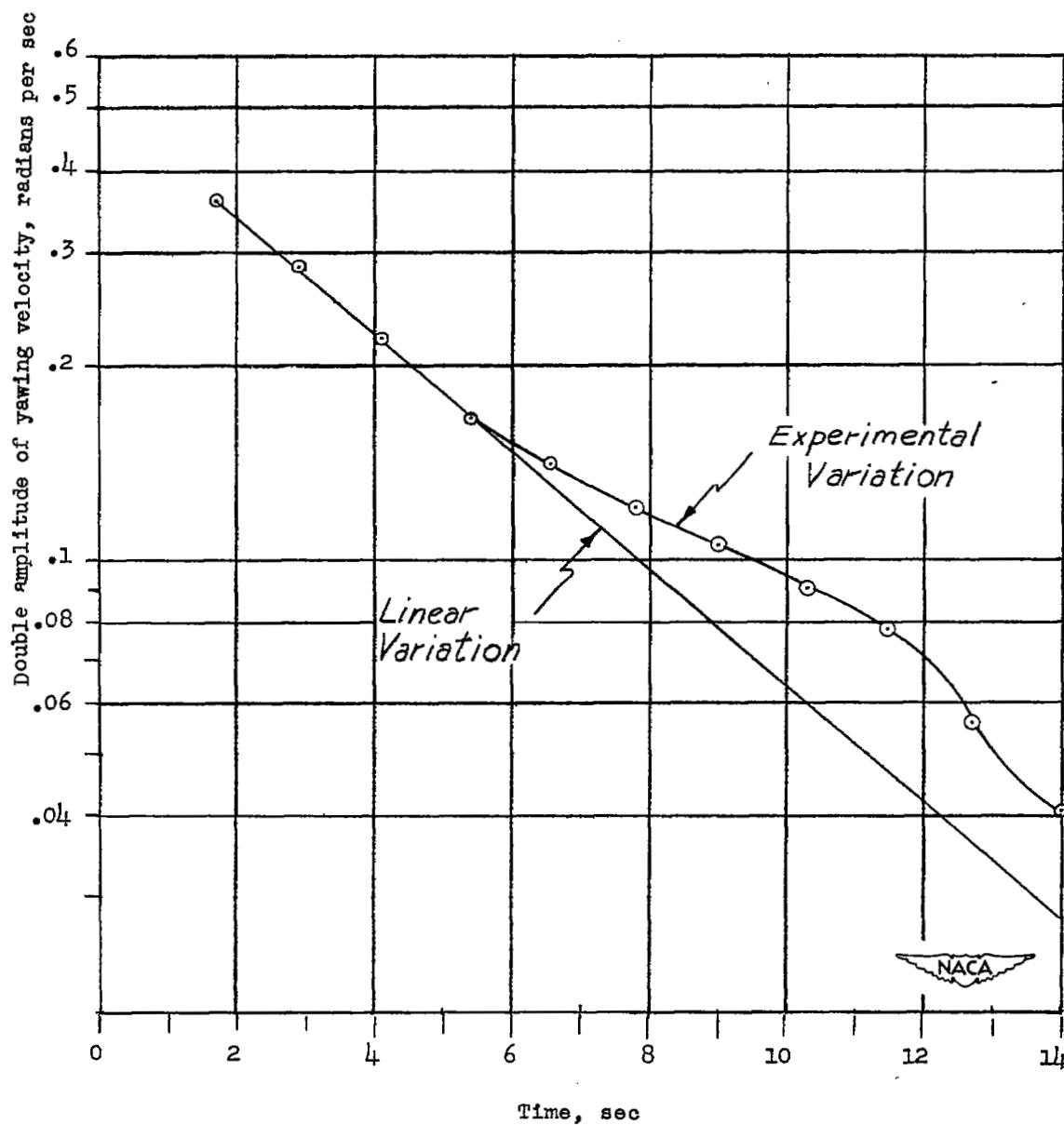
Figure 5.- Variation of double amplitude of yawing velocity with time
during a controls-free lateral oscillation of the test airplane.
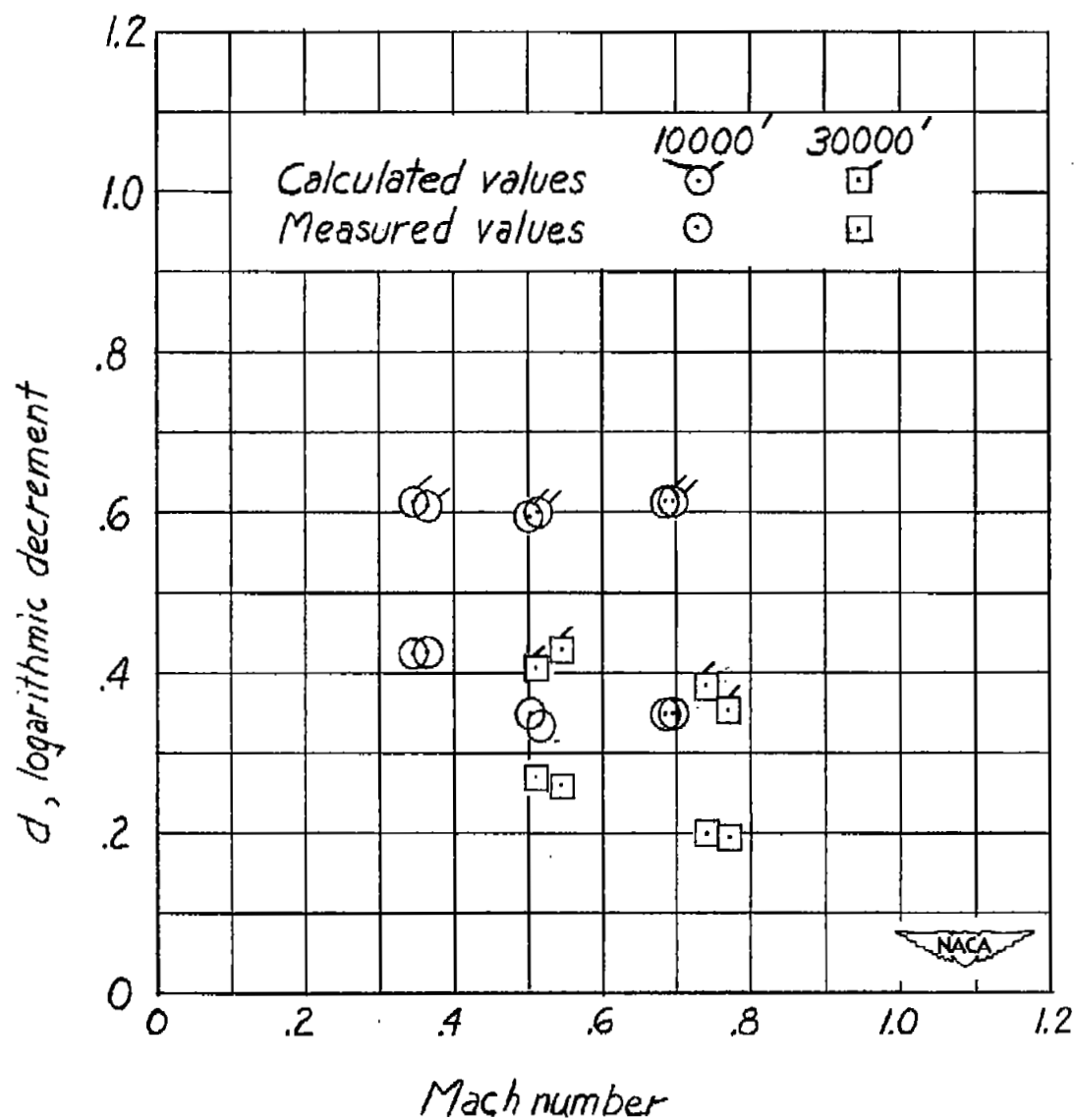
Figure 6.- Comparison of the calculated controls-fixed damping with the measured controls-free damping of the lateral oscillation.
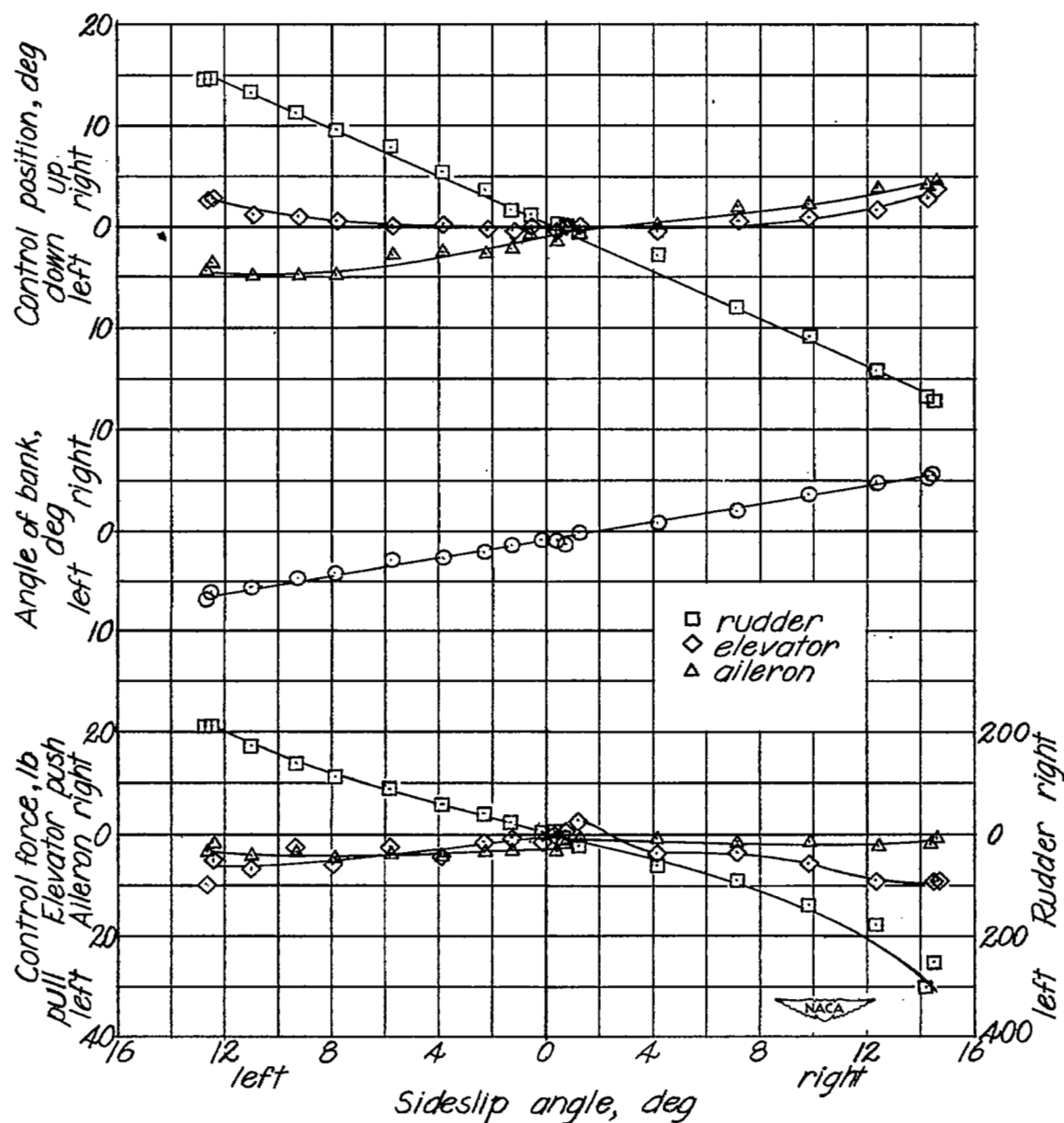
(a) V_i = 142 miles per hour; h_p = 10,000 feet; M = 0.22.

Figure 7.- Sideslips in the clean condition measured at two test altitudes
of 10,000 and 30,000 feet.
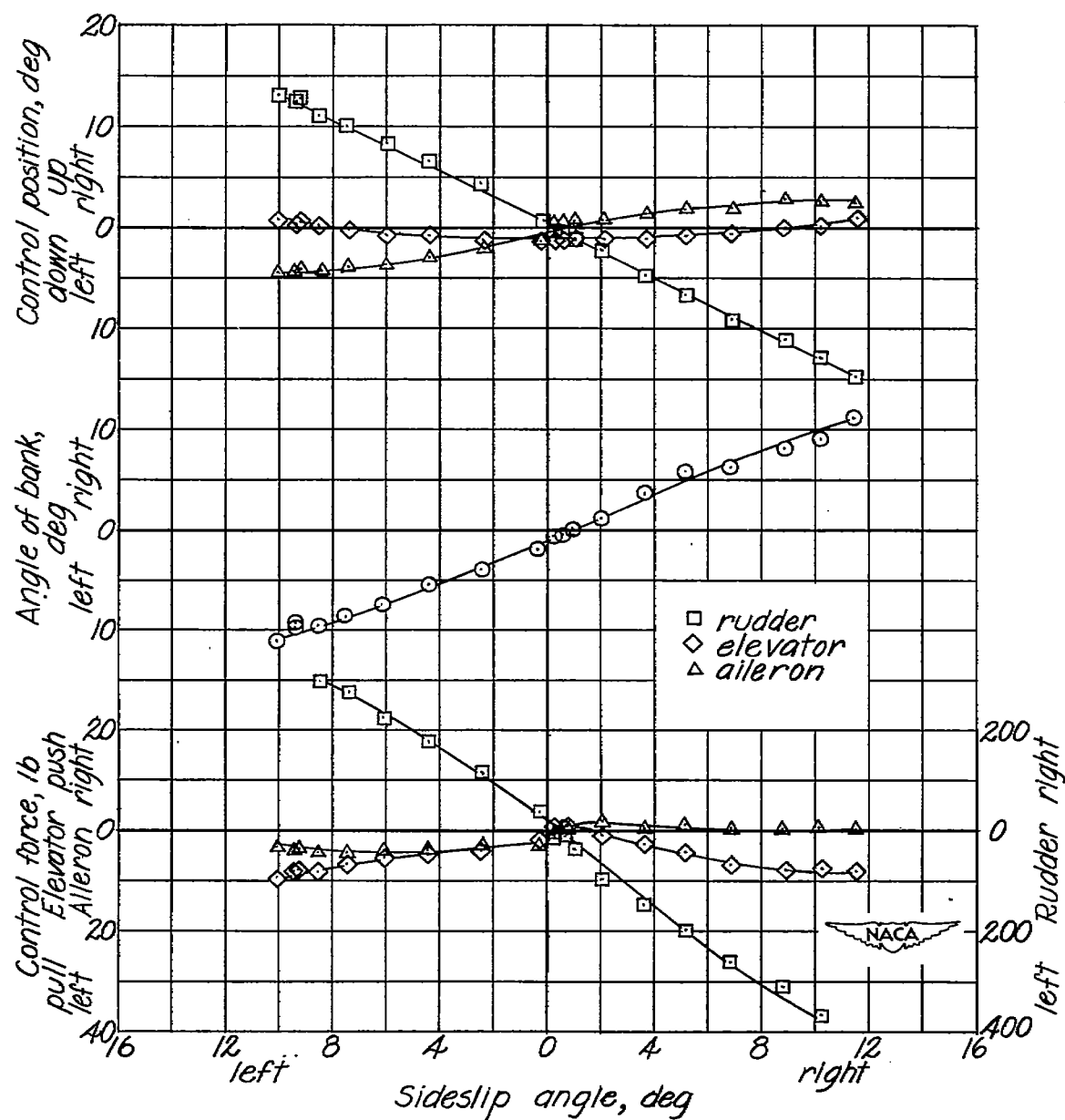
(b) V_i = 231 miles per hour; h_p = 10,600 feet; M = 0.37.

Figure 7.- Continued.
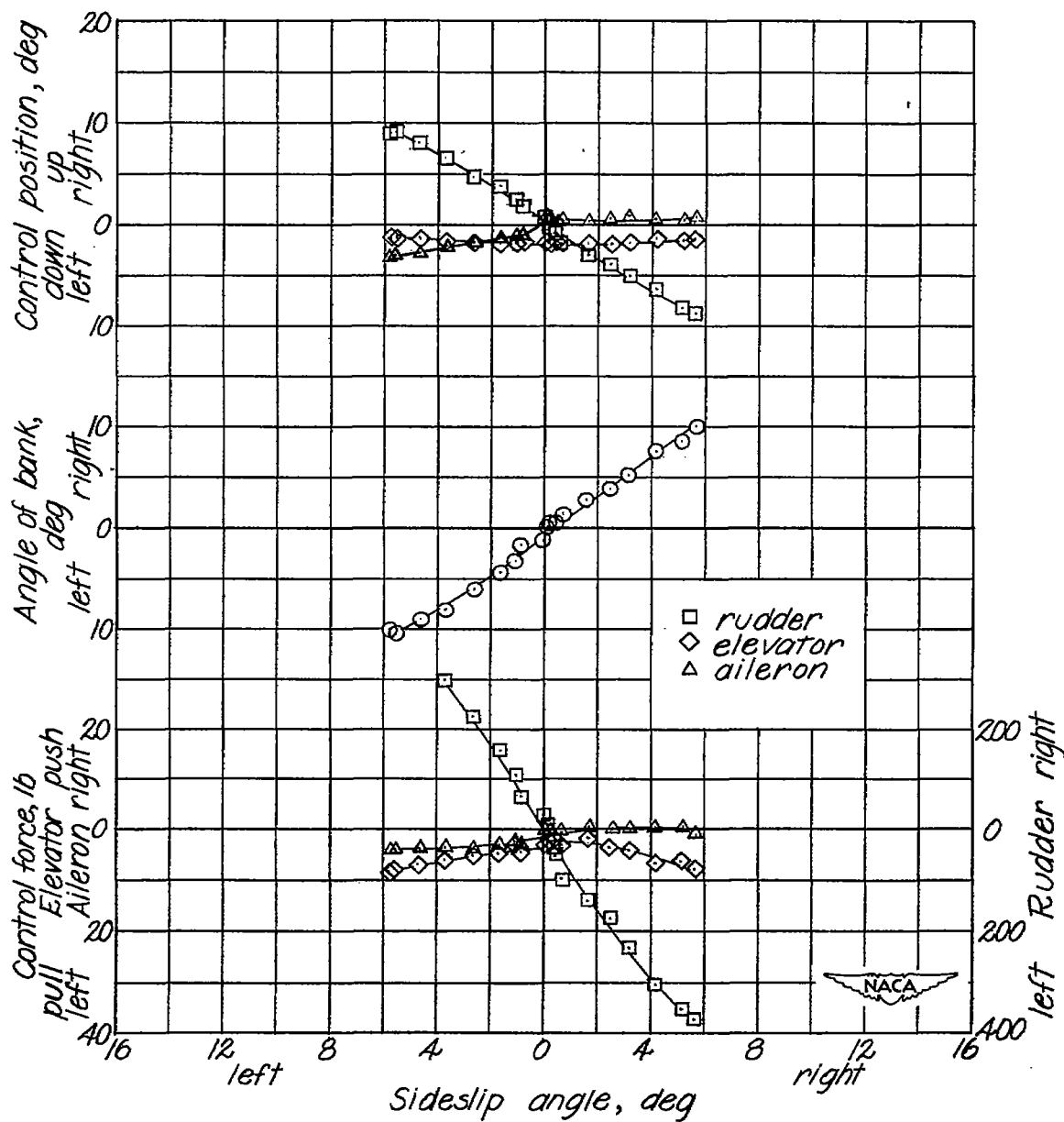
(c) V_i = 311 miles per hour; h_p = 9,700 feet; M = 0.49.

Figure 7.- Continued.
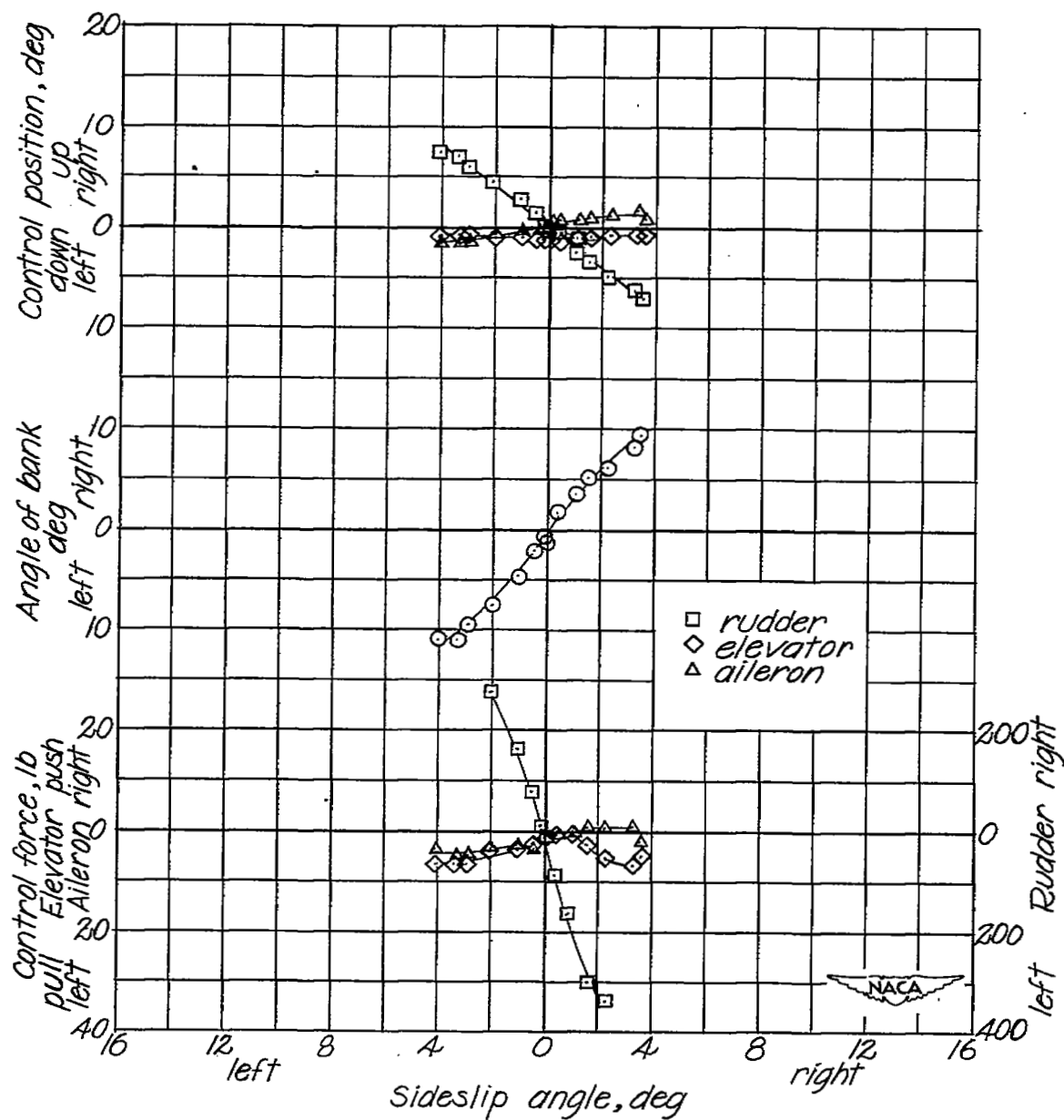
(d) V_i = 394 miles per hour; h_p = 9,200 feet; M = 0.61.

Figure 7.- Continued.
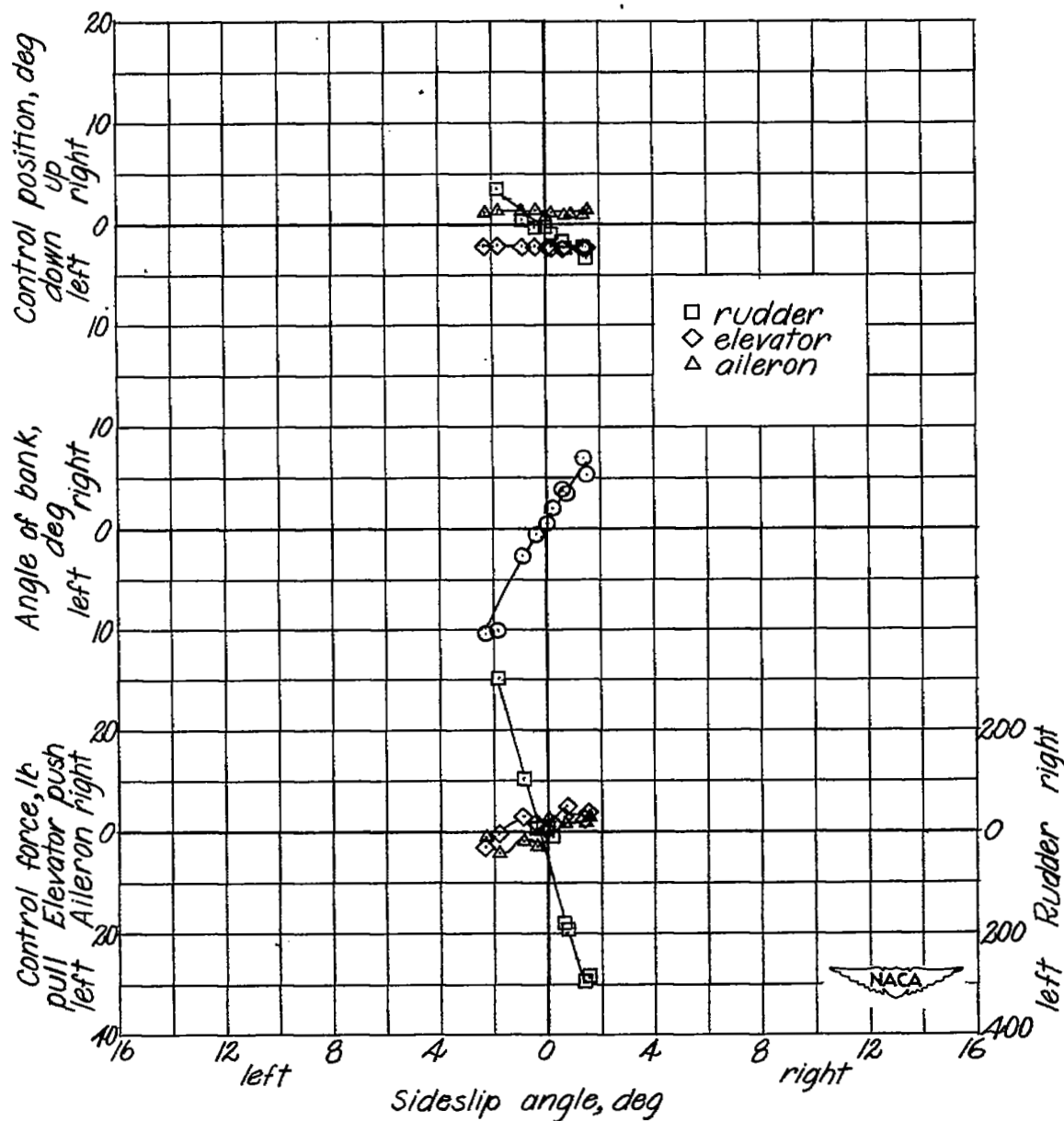
(e) V_i = 468 miles per hour; h_p = 9,700 feet; M = 0.715.

Figure 7.- Continued.
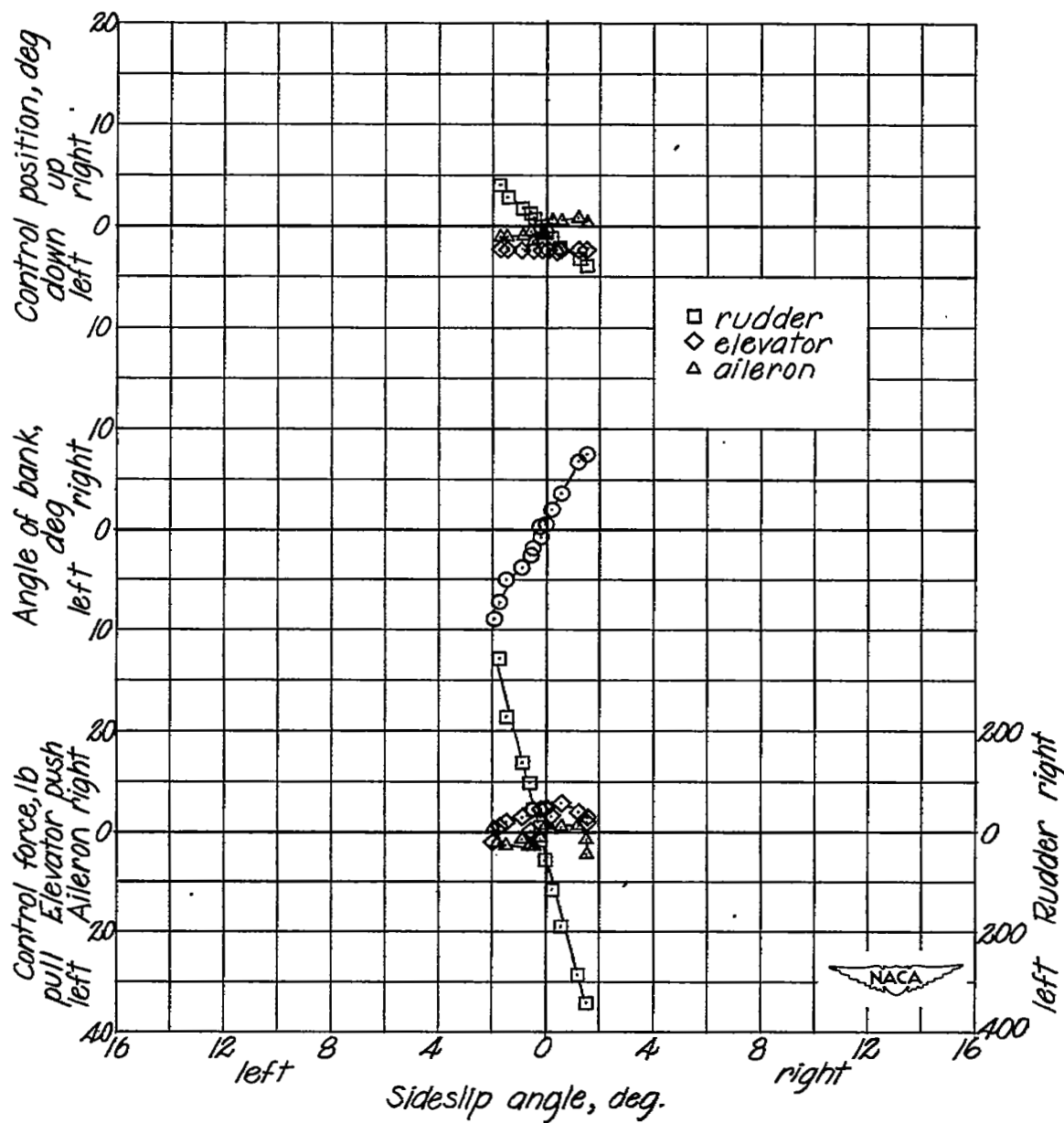
(f) V_i = 483 miles per hour; h_p = 8,800 feet; M = 0.74.

Figure 7.- Continued.
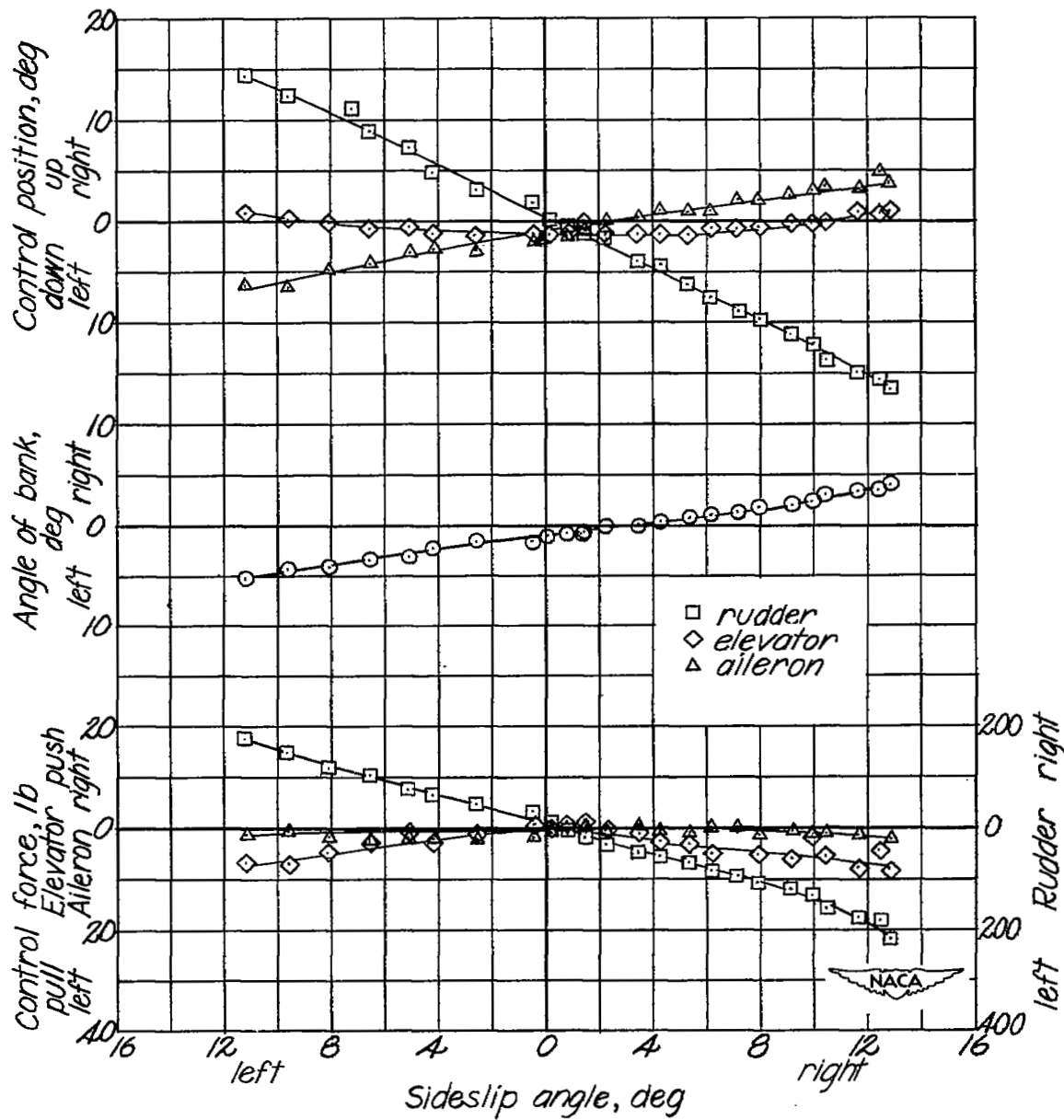
(g)　$V_i = 139$ miles per hour; $h_p = 29{,}500$ feet; $M = 0.33$.

Figure 7.- Continued.
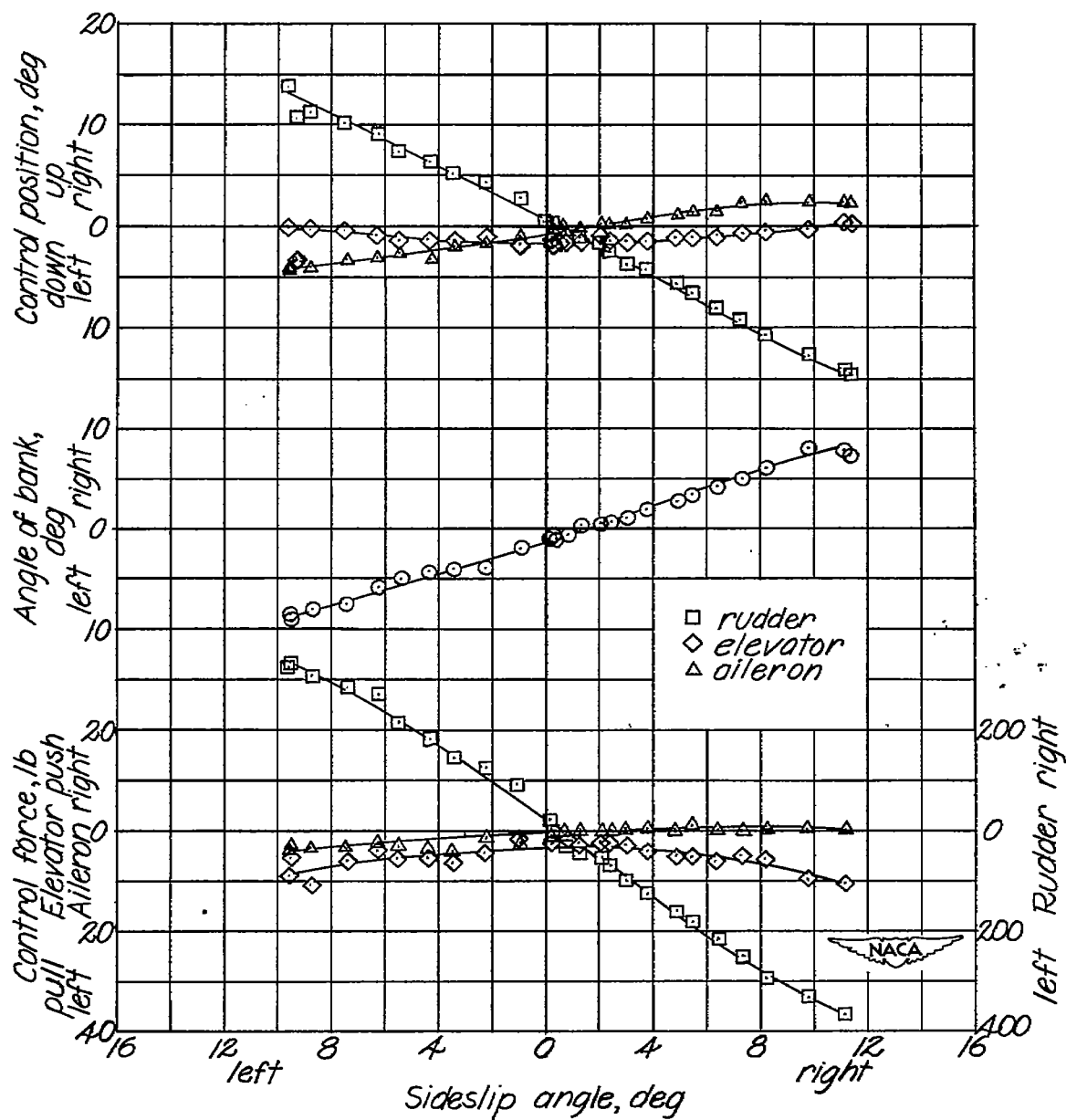
(h) V_i = 232 miles per hour; h_p = 29,300 feet; M = 0.54.

Figure 7.- Continued.
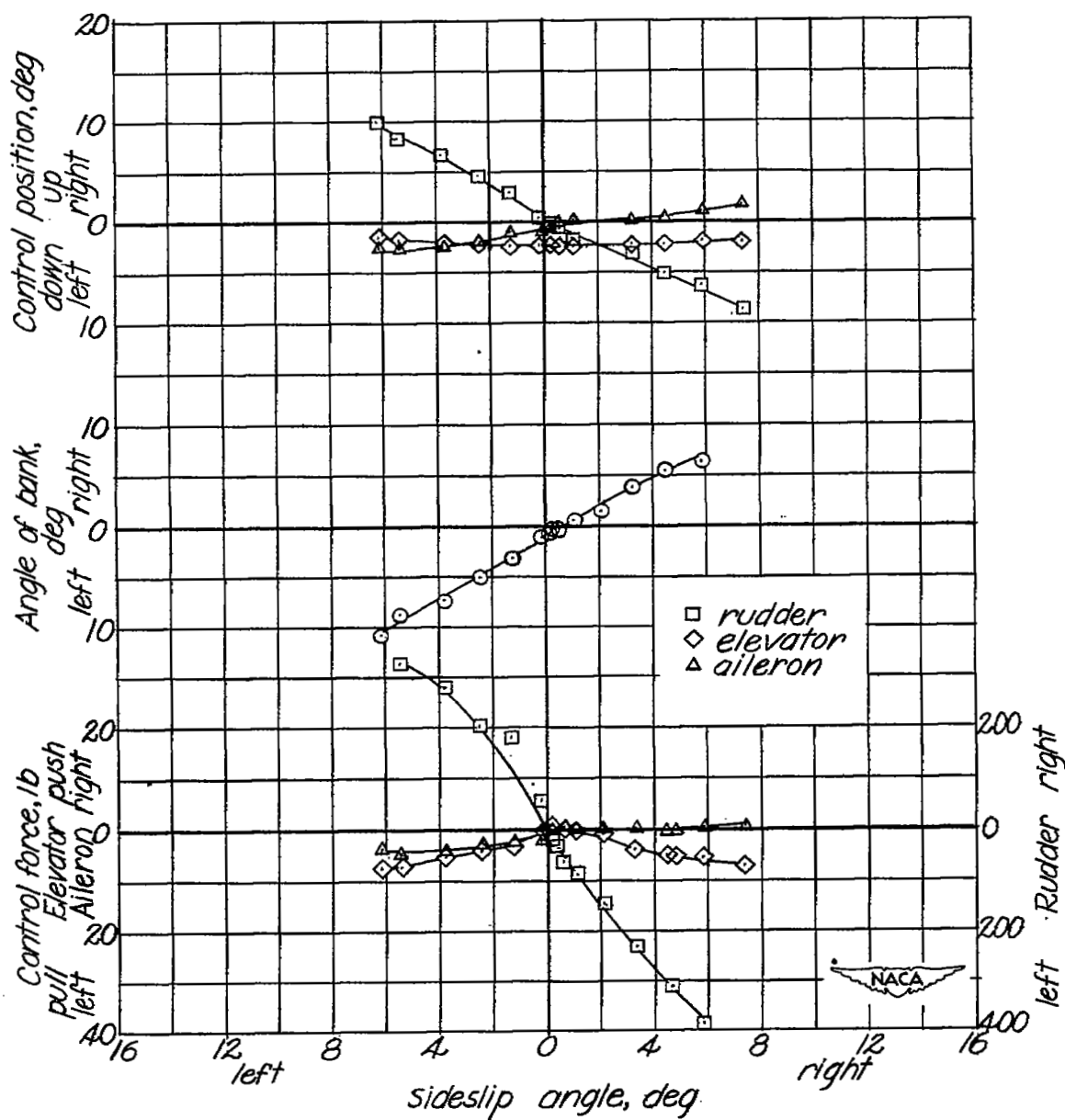
(i) V_i = 310 miles per hour; h_p = 29,900 feet; M = 0.71.

Figure 7.- Continued.
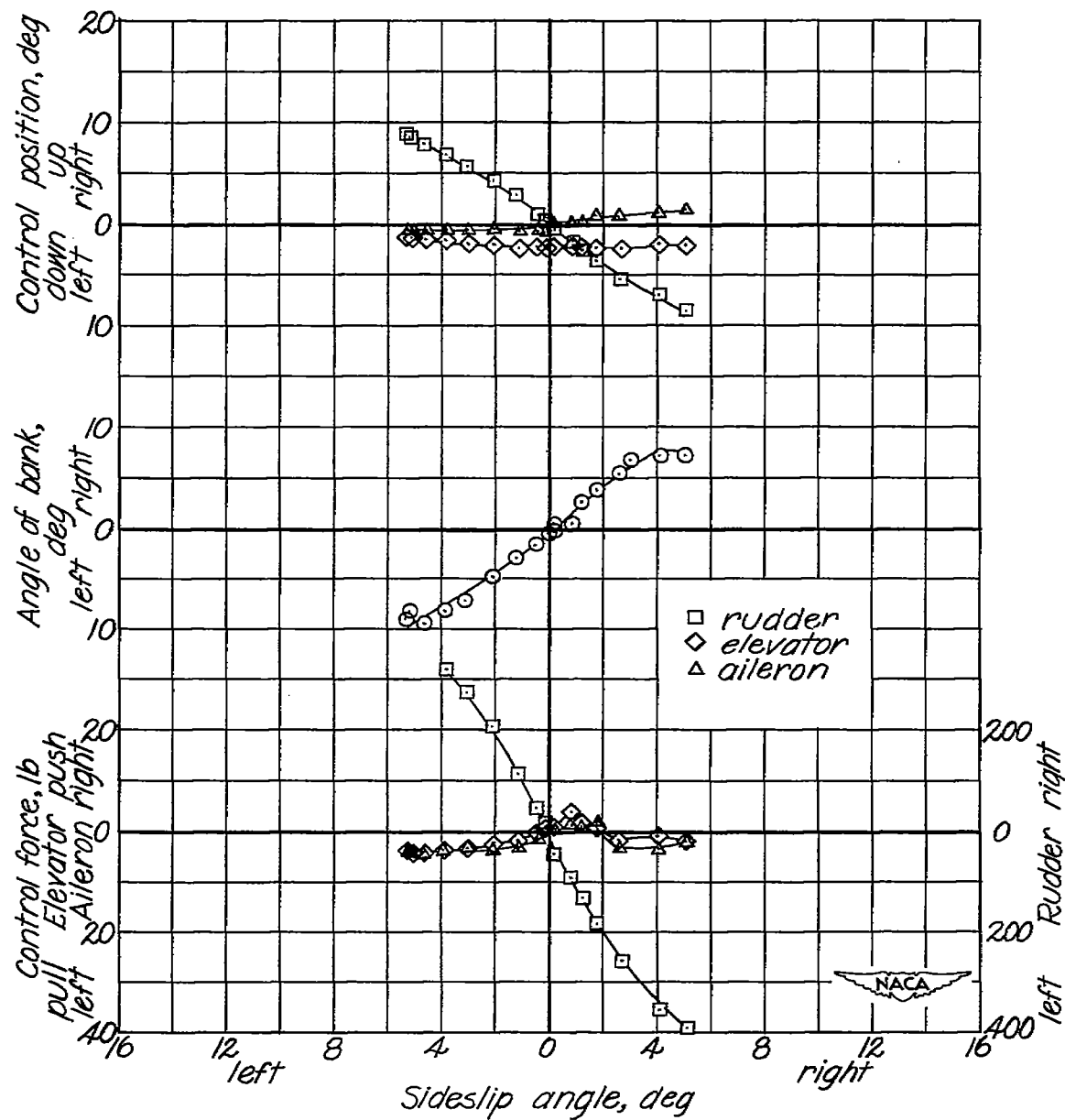
(j) V_i = 336 miles per hour; h_p = 29,100 feet; M = 0.76.

Figure 7.- Continued.

NACA RM L52B14
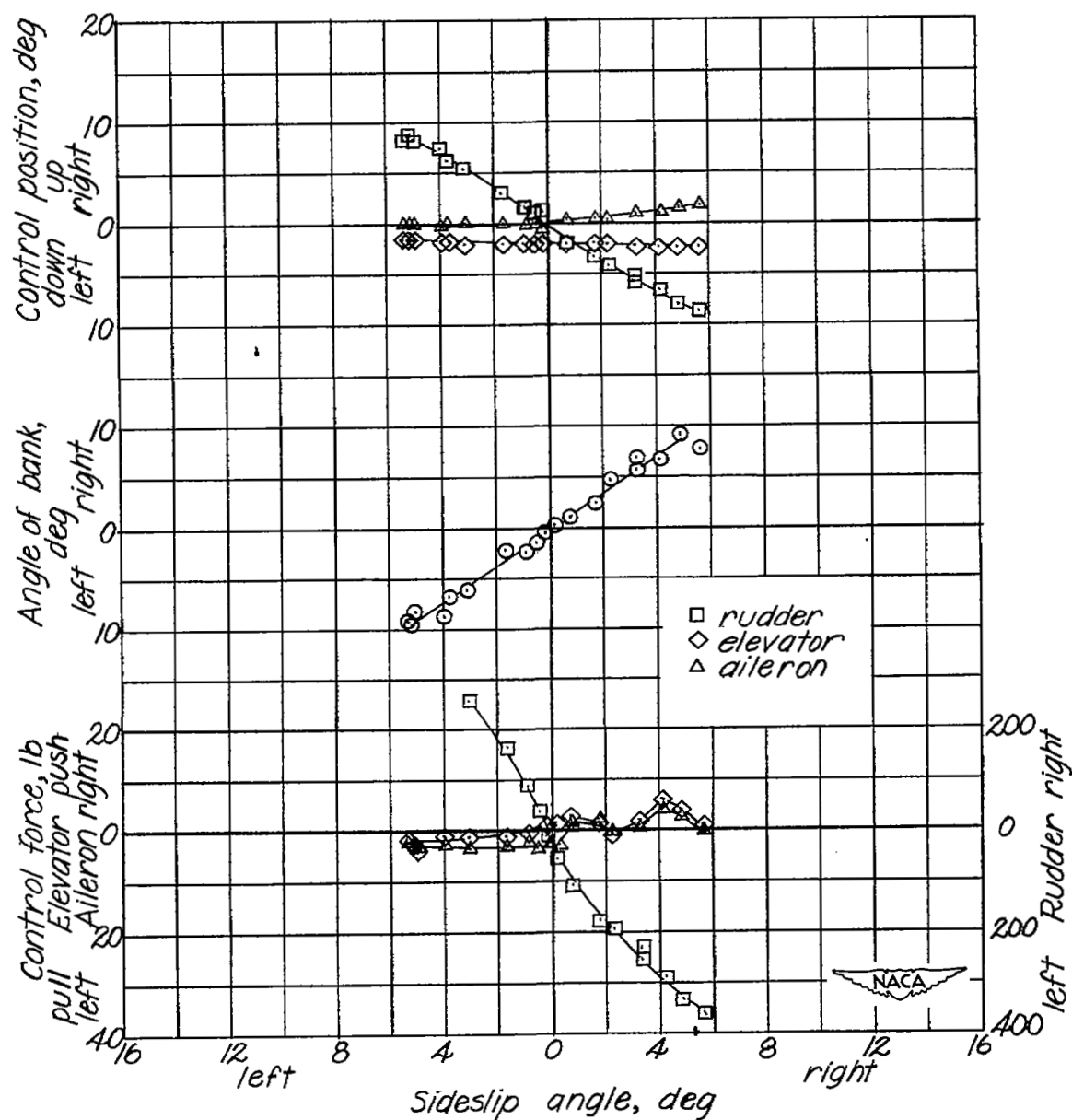
(k) V_1 = 347 miles per hour; h_p = 29,200 feet; M = 0.78.

Figure 7.- Continued.
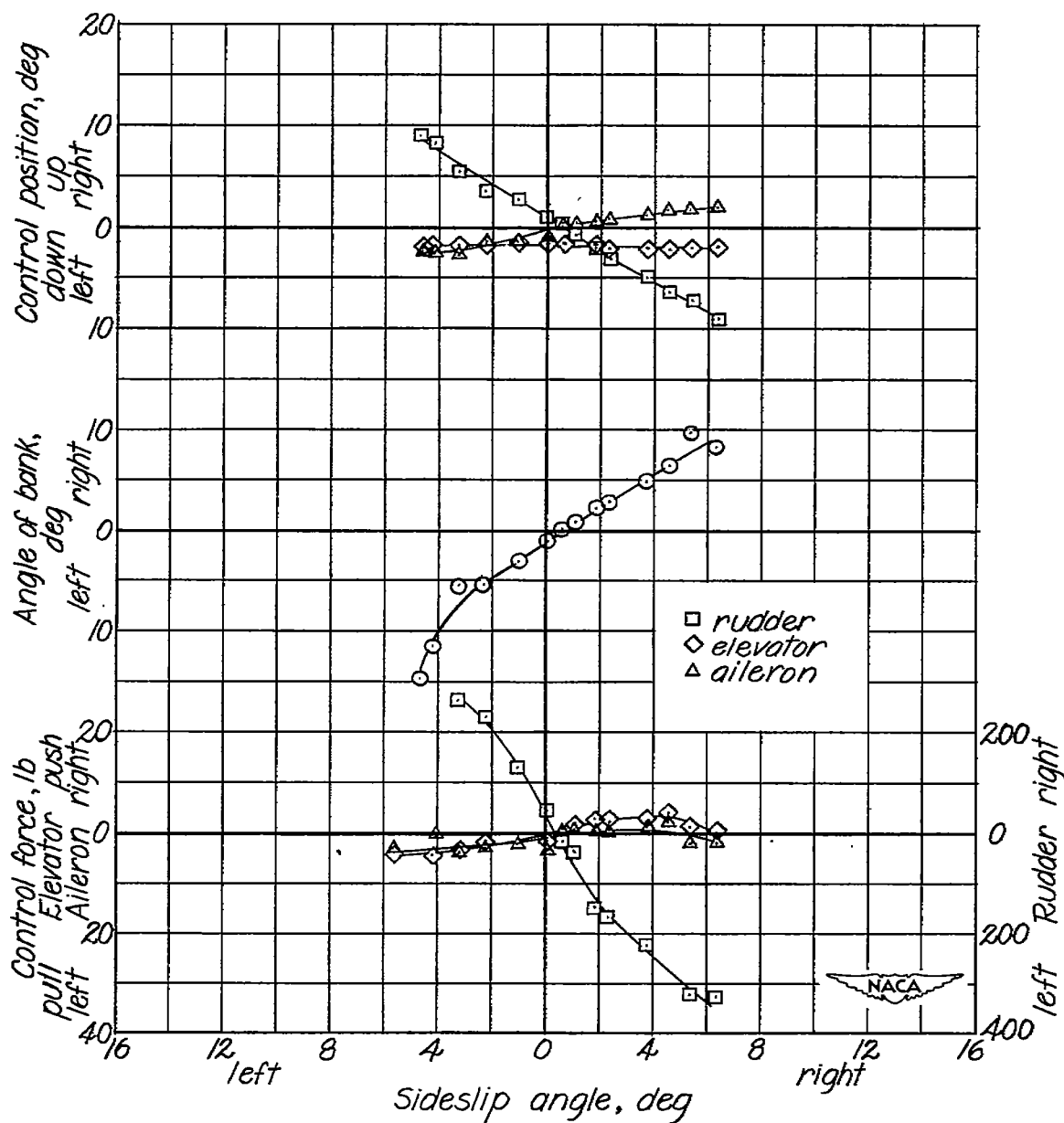
(*l*) V_i = 354 miles per hour; h_p = 29,000 feet; M = 0.79.

Figure 7.- Continued.
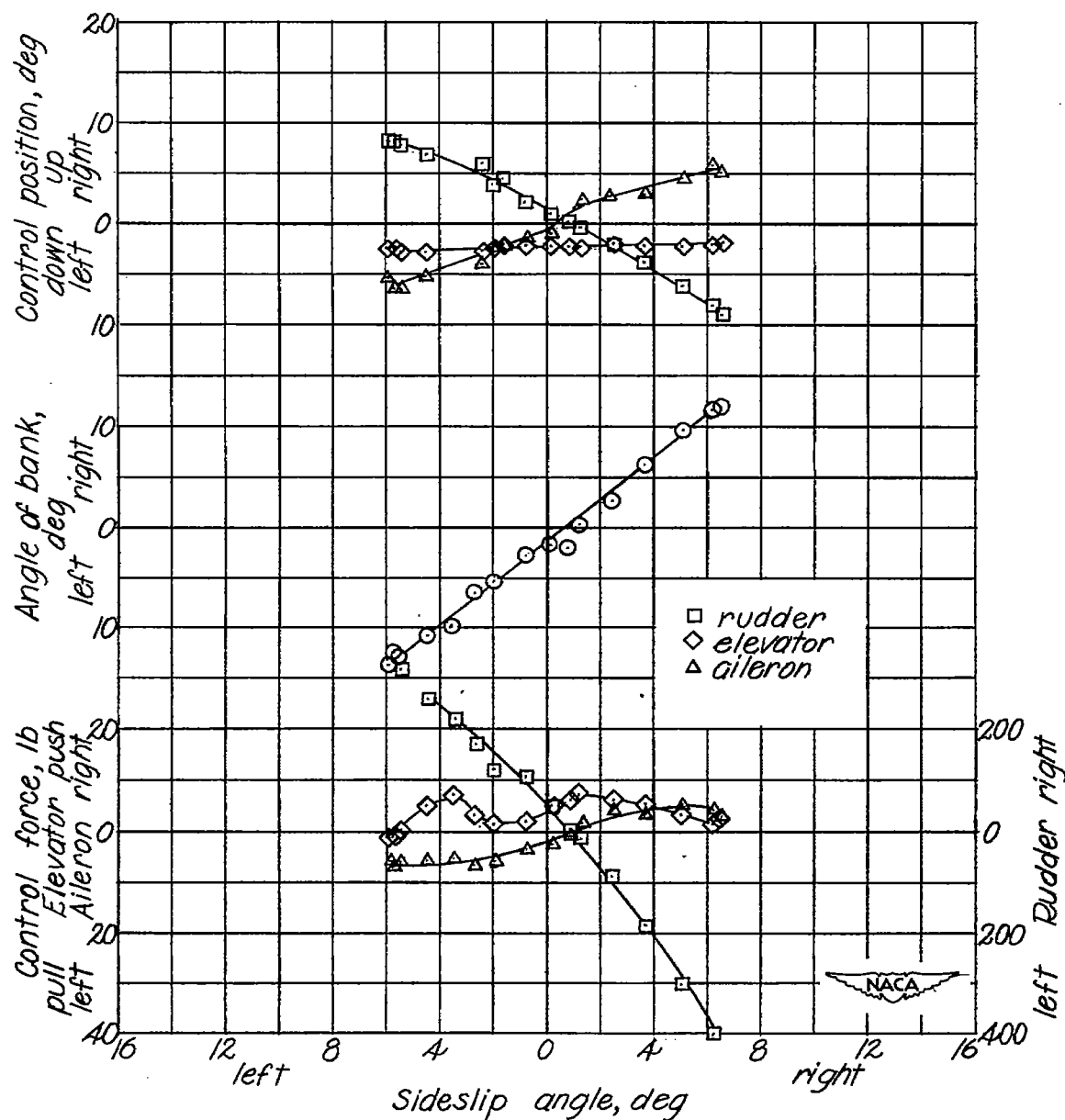
(m) $V_i = 374$ miles per hour; $h_p = 28,600$ feet; $M = 0.83$.

Figure 7.- Continued.
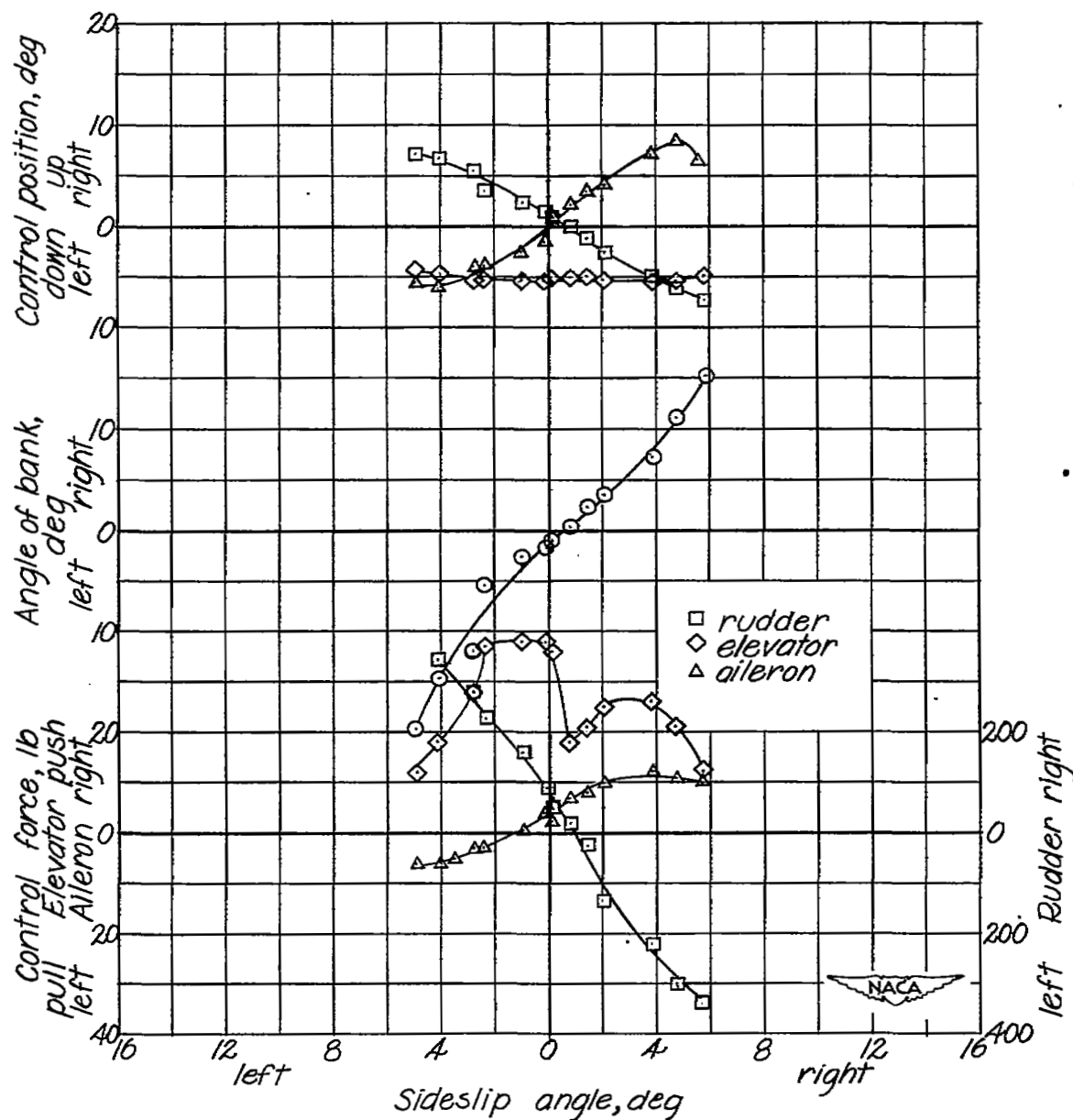
(n) V_i = 381 miles per hour; h_p = 28,200 feet; M = 0.84.

Figure 7.- Concluded.
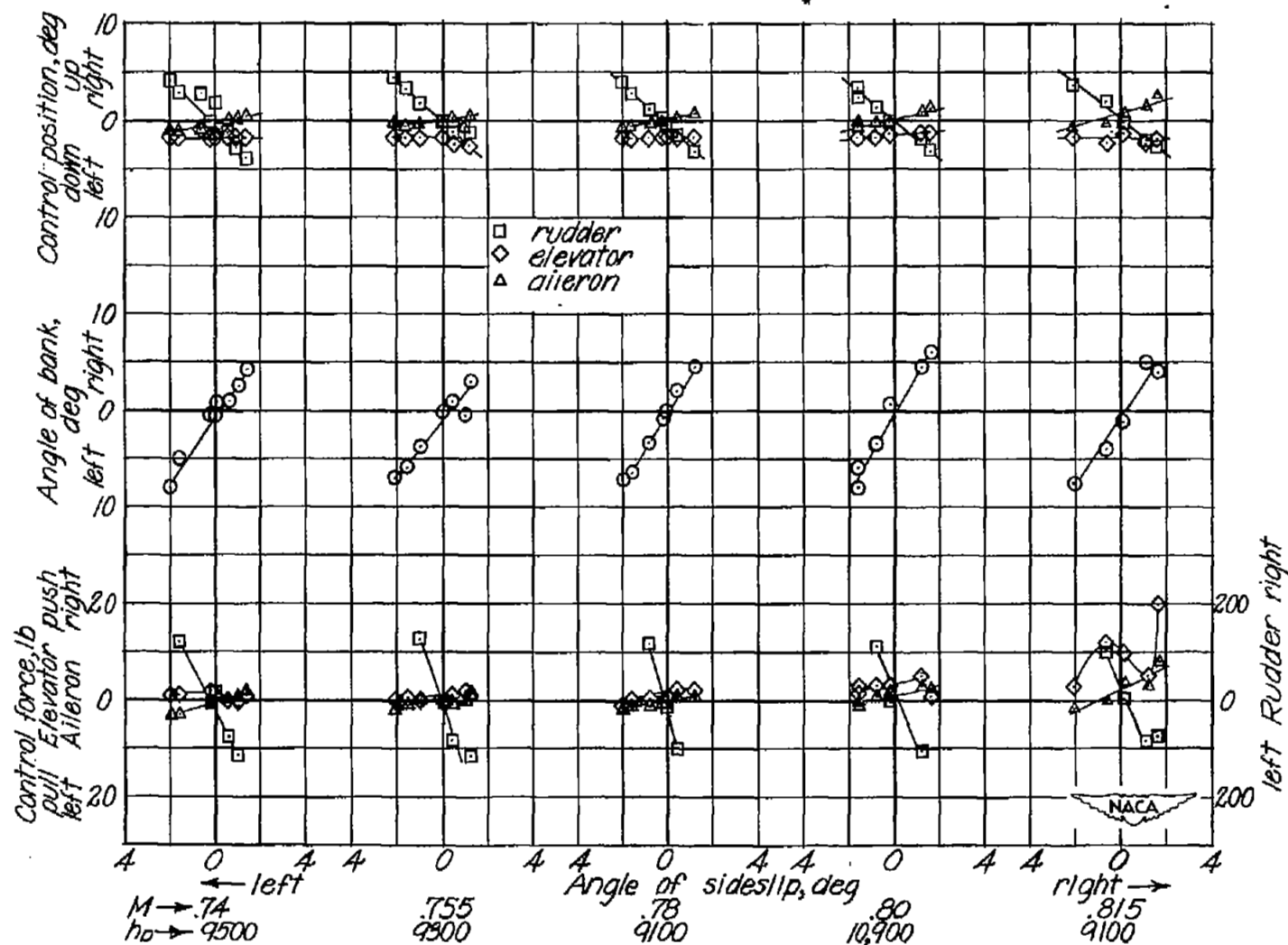
Figure 8.- Sideslip characteristics in the clean condition from spot records of steady sideslips.
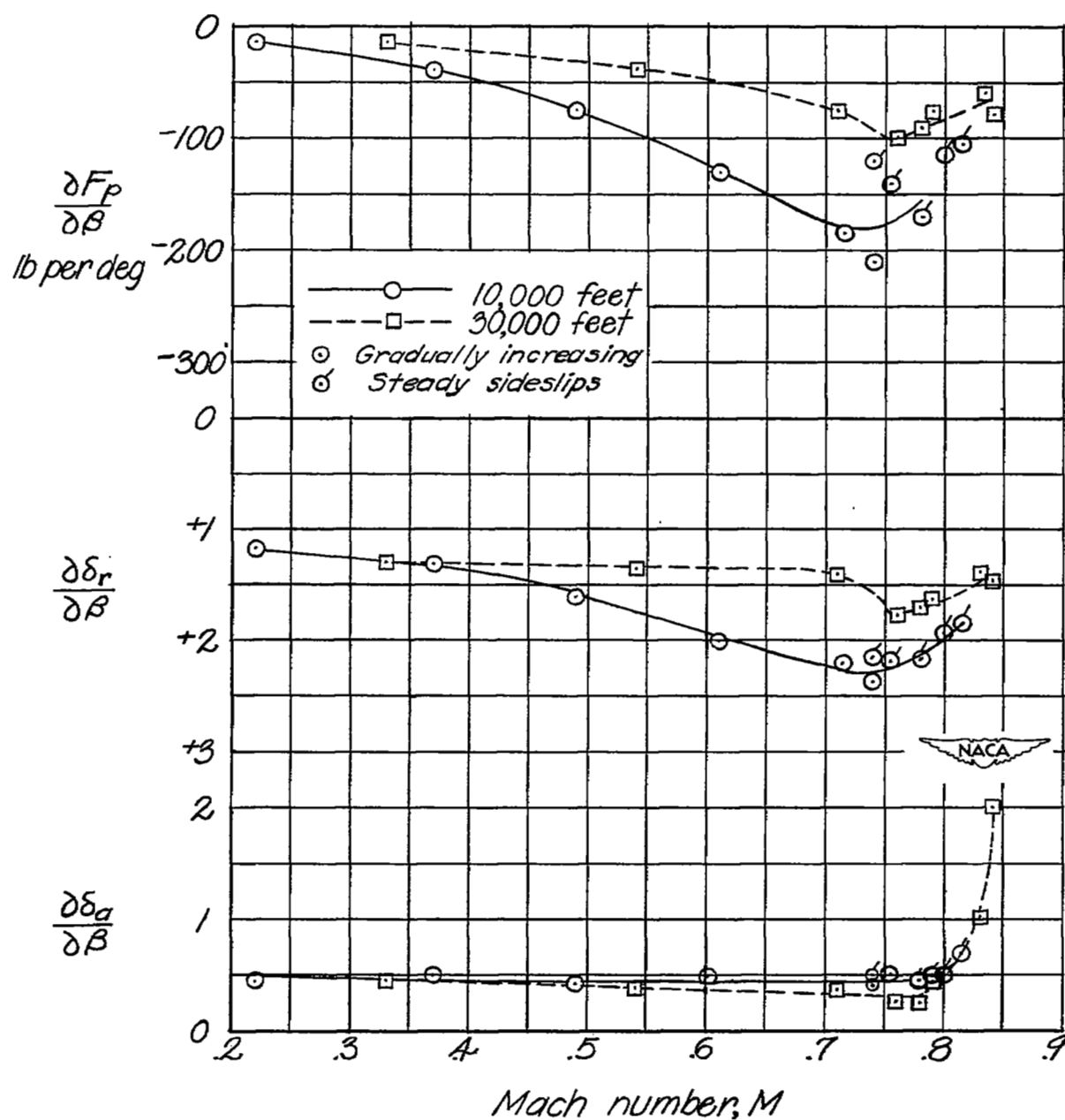
(a) With Mach number.

Figure 9.- Variation of $\partial F_p/\partial\beta$, $\partial\delta_r/\partial\beta$, and $\partial\delta_a/\partial\beta$ with Mach number and dynamic pressure.
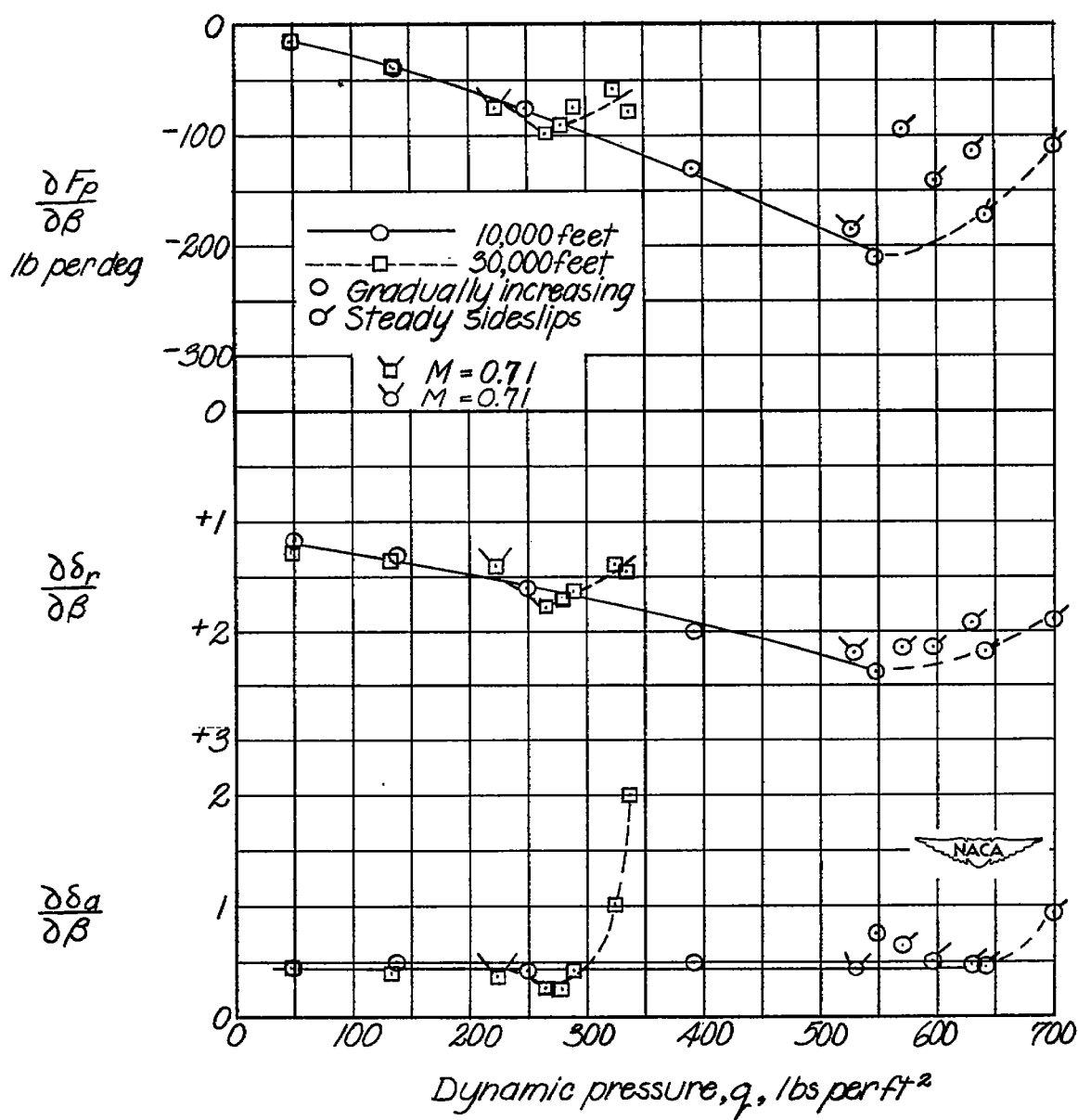
(b) With dynamic pressure.

Figure 9.- Concluded.
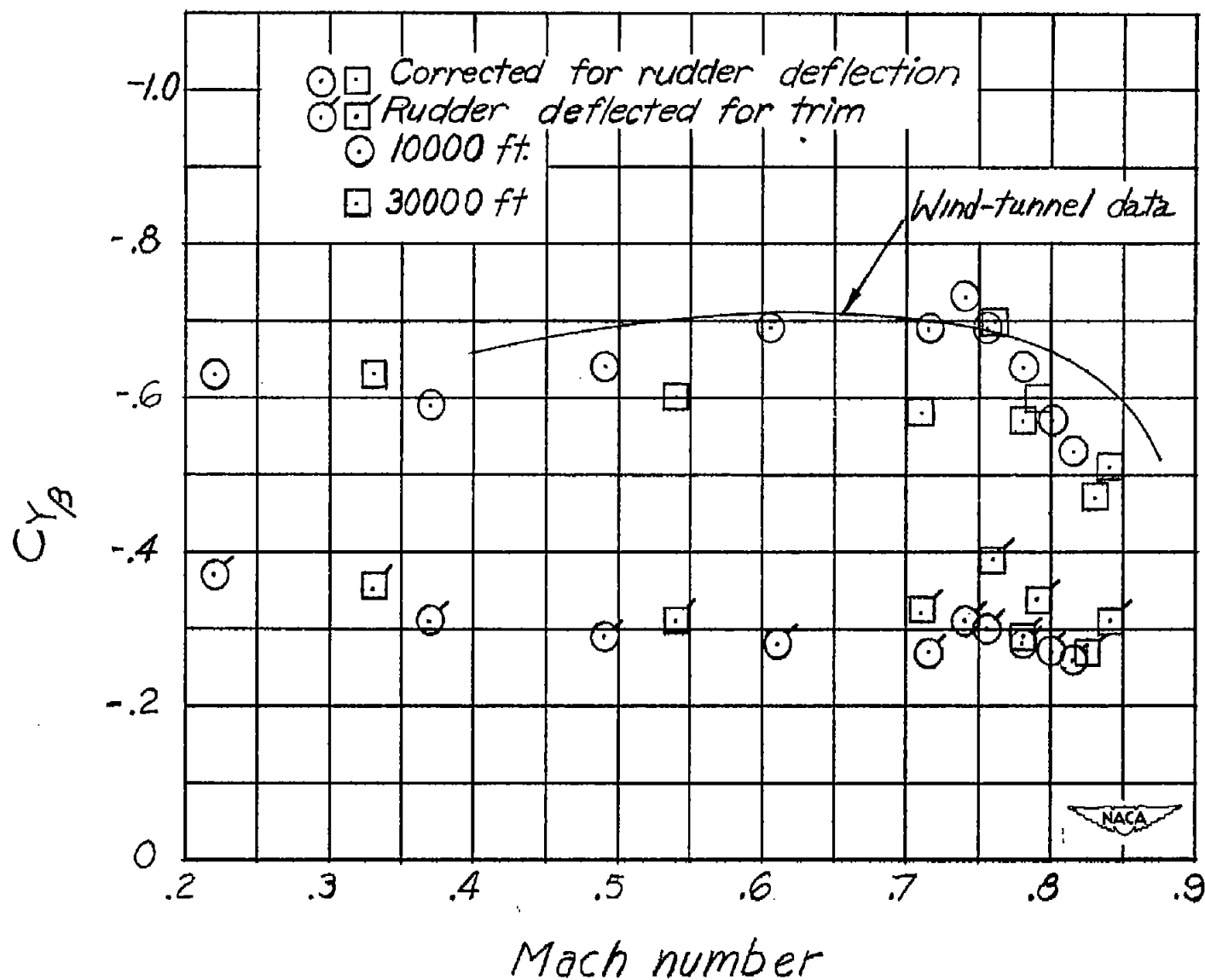
Figure 10.- Variation of the side-force derivative C_{Y_β} with Mach number.
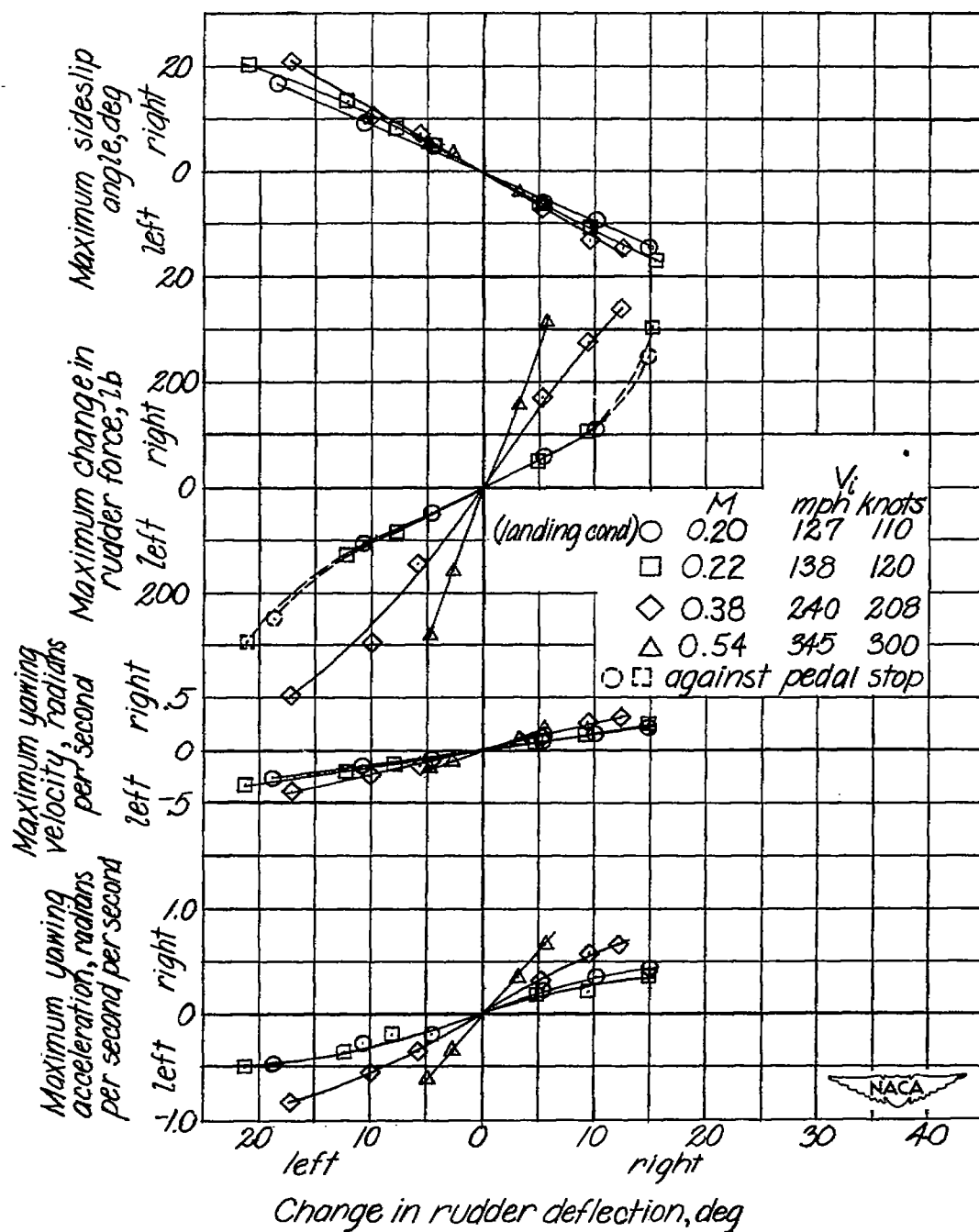
(a) 10,000 feet.

Figure 11.- Rudder-control characteristics of the test airplane measured
in abrupt rudder kicks in the clean condition.
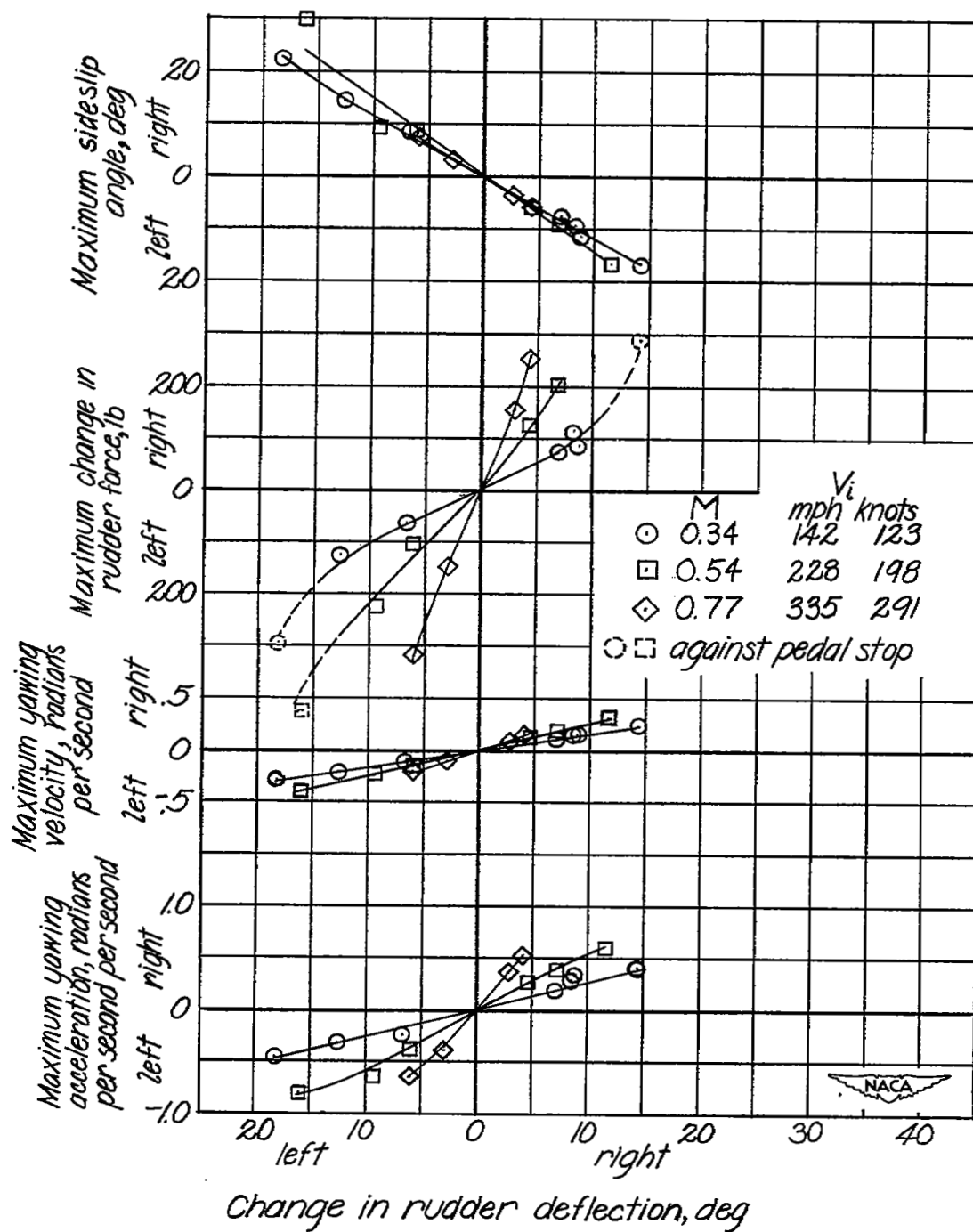
(b) 30,000 feet.

Figure 11.- Concluded.
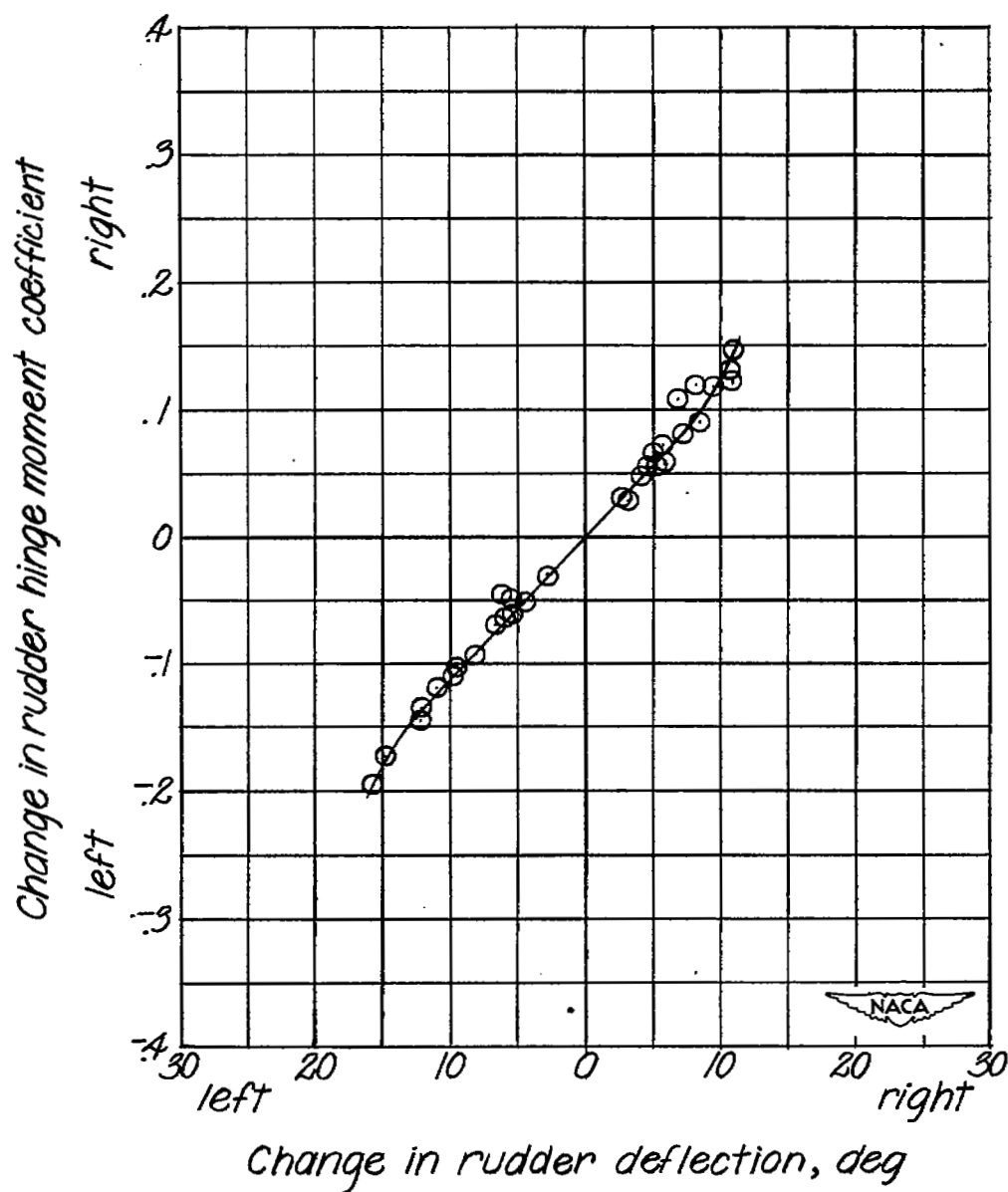
(a) Change in rudder hinge moment due to change in rudder deflection.

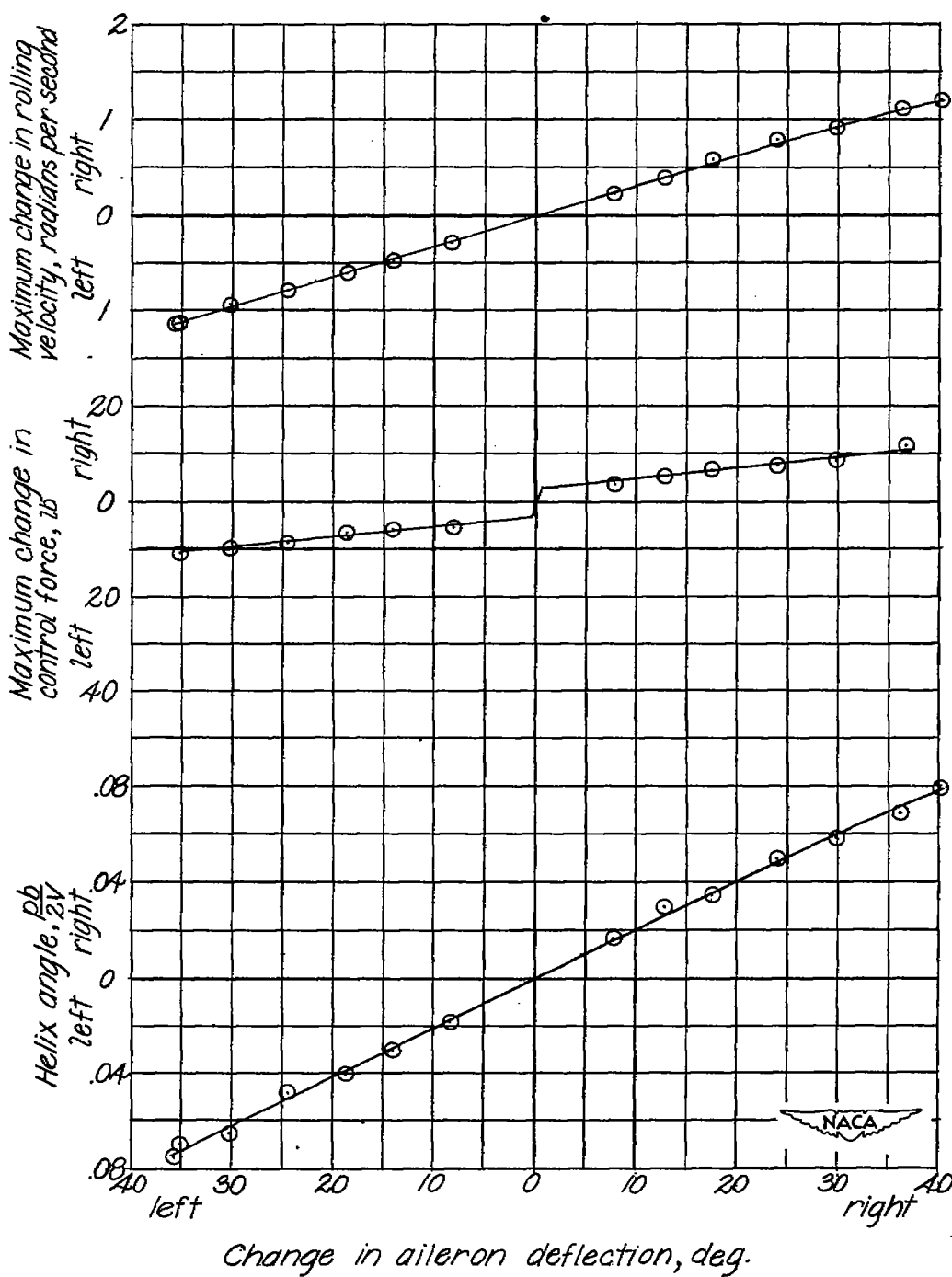Figure 12.- Rudder hinge-moment characteristics measured at 10,000 and 30,000 feet. (Unbalancing tab ratio 1.4:1.)
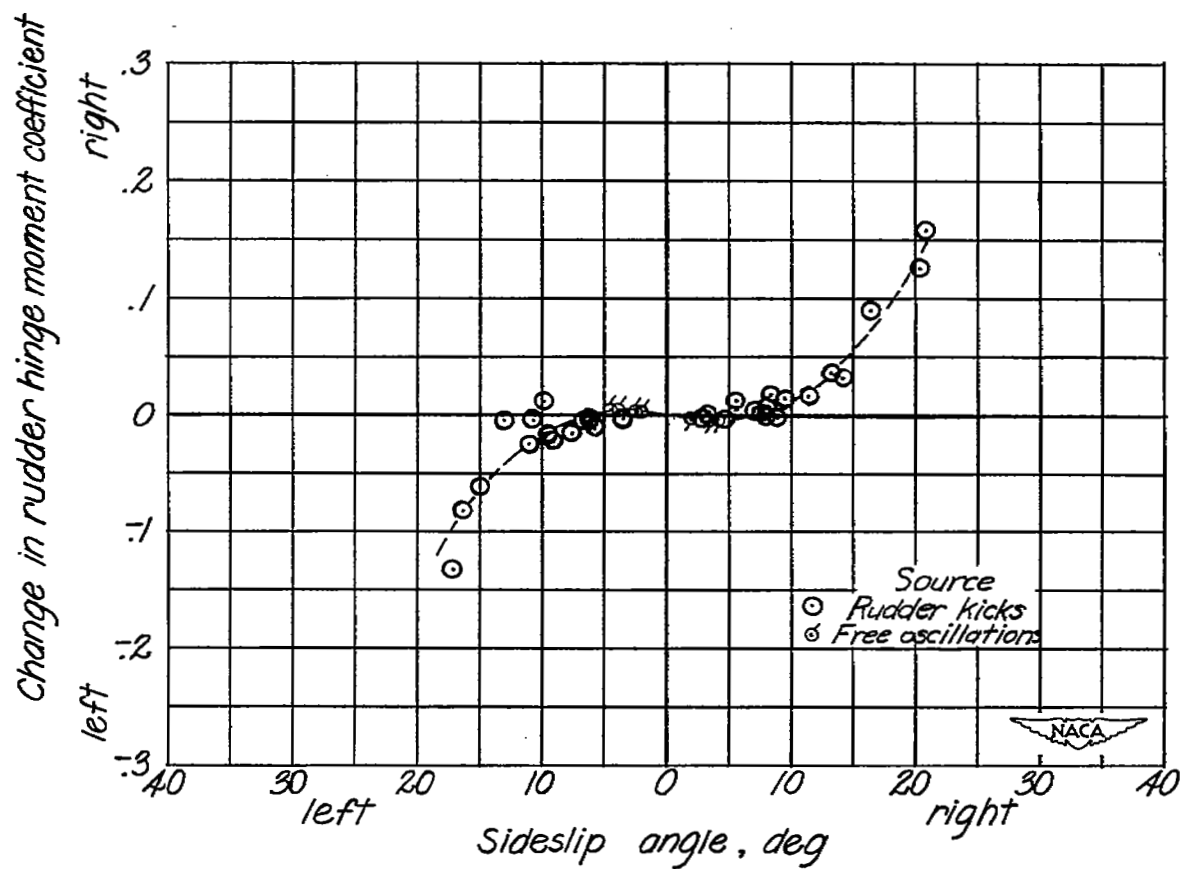
(b) Change in rudder hinge moment due to sideslip angle.
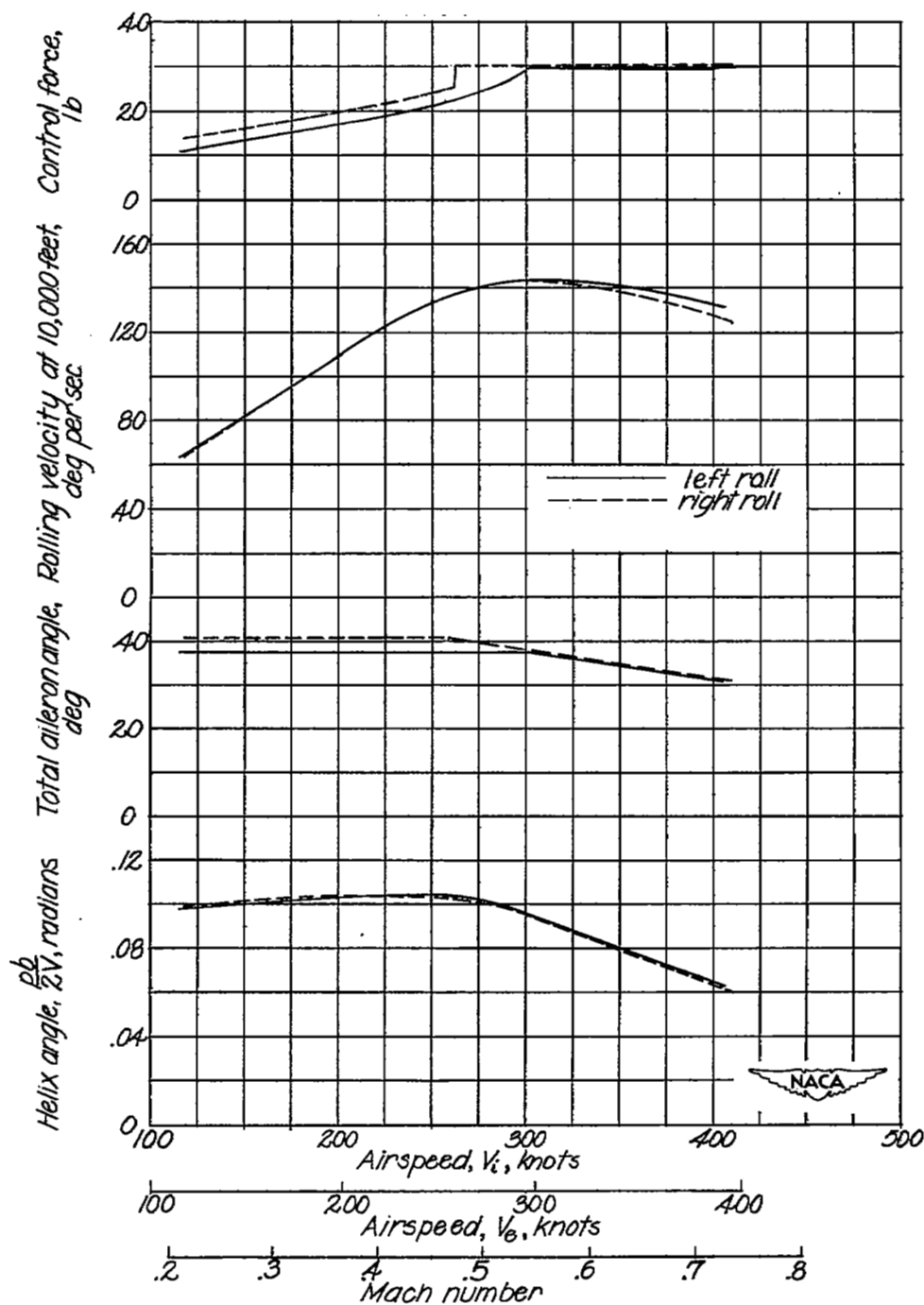
Figure 12.- Concluded.

(a) 10,000 feet.

Figure 13.- Rolling characteristics of the test airplane measured in
abrupt aileron rolls from wings level flight.

Change in aileron deflection, deg.
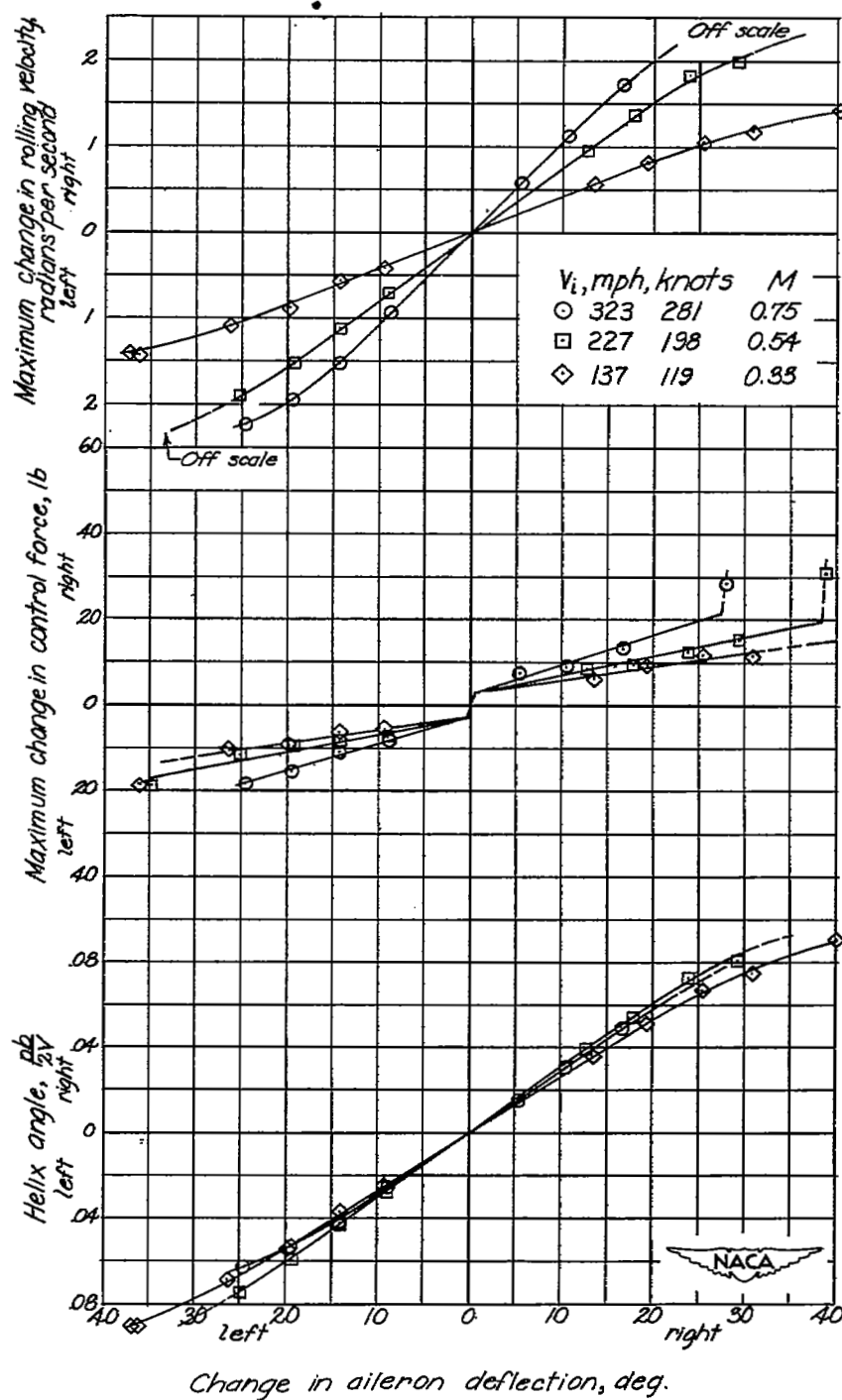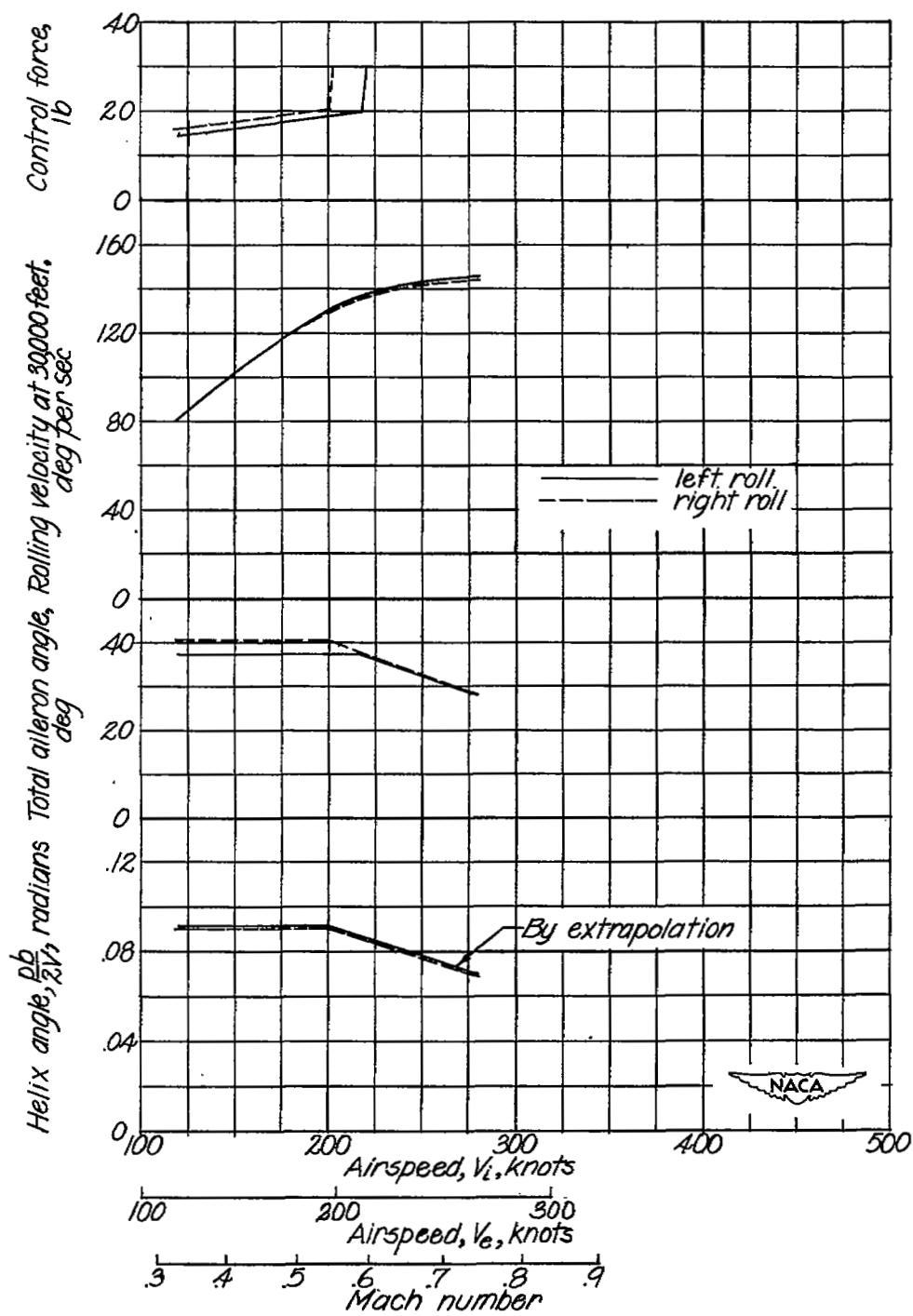
(b) 30,000 feet.

Figure 13.- Continued.

(c) Landing condition, 205 miles per hour (178 knots) at an altitude of 5,000 feet.

Figure 13.- Concluded.

(a) 10,000 feet.

Figure 14.- Variation of control force, rolling velocity, total aileron
angle, and helix angle with airspeed measured in abrupt aileron rolls
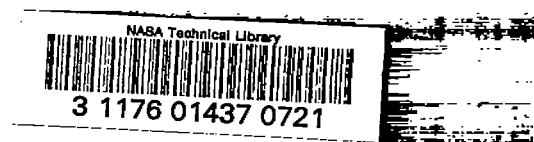from wings level flight.

(b)   30,000 feet.

Figure 14.- Concluded.